Abstract

In this study we present an improved Cenozoic stratigraphy of the Biga Peninsula, NW Anatolia, derived from a comprehensive set of U-Pb zircon age data obtained from the Eocene to Lower Miocene volcanic units in the region. The timing of extension, granitic magmatism and volcanic activity of the Biga region are then compared and correlated with the northwesterly located Rhodope and Thrace and the easterly located Armutlu-Almacık-Nallıhan regions. The compiled radiometric age data show that calc-alkaline volcanic activity occurred at ~43-15 Ma in the Biga Peninsula, ~43-17 Ma in the Rhodope and Thrace regions, and ~53-38 Ma in the Armutlu-Almacık-Nallıhan region. We discuss the possible cause for the distinct Cenozoic geodynamic evolution of the eastern and western parts of the region, and propose that the Rhodope, Thrace and Biga regions in the north Aegean share the same Late Mesozoic to Cenozoic geodynamic evolution, which is consistent with continuous subduction, crustal accretion, southwestward trench migration and accompanying extension; all preceded by the Late Cretaceous – Paleocene collision along the Vardar suture zone. In contrast, the Armutlu-Almacık-Nallıhan region that lies to the east was shaped by slab break-off and related processes following the Late Cretaceous – Paleocene collision along the İzmir-Ankara suture zone. The eastern and western parts of the region are presently separated by a northeast-southwest trending transfer zone that was likely originally present as a transform fault in the subducted Tethys oceanic crust, and demonstrates that the regional geodynamic evolution can be strongly influenced by the geographical distribution of geologic features on the subducting plate.

Highlights

- U-Pb zircon ages of the Biga Peninsula volcanics are measured
- Tectono-magmatic evolution of the region investigated.
- Tectonic evolution of the Rhodope to Anatolia is compared
- Cenozoic geodynamics of the Aegean is discussed

U-Pb zircon Geochronology of the Paleogene – Neogene Volcanism in the NW Anatolia: Its implications for the Late Mesozoic-Cenozoic Geodynamic Evolution of the Aegean

E. Yalçın Ersoy* [(1)], Cüneyt Akal[(1)], Ş. Can Genç[(2)], Osman Candan[(1)], Martin R. Palmer[(3)], Dejan Prelević[(4,5)], İbrahim Uysal[(6)], Regina Mertz-Kraus[(4)]

[(1)] Dokuz Eylül University, Dept. of Geological Engineering, TR-35160, İzmir, Turkey

[(2)] İstanbul Technical University, Dept. of Geological Engineering, TR-34469 İstanbul, Turkey

[(3)] School of Ocean and Earth Science, University of Southampton, National Oceanography Centre, European Way, Southampton SO14 3ZH, UK

[(4)] Institute for Geosciences, Johannes Gutenberg University, 55099 Mainz, Germany

[(5)] Faculty of Mining and Geology University, Belgrade, Serbia

[(6)] Karadeniz Technical University, Dept. of Geological Engineering TR-61080 Trabzon, Turkey

[(*)] **Corresponding author**:

Dr. E. Yalçın Ersoy
e-mail: yalcin.ersoy@deu.edu.tr
Tel: +90 (232) 301 73 46

Abstract

In this study we present an improved Cenozoic stratigraphy of the Biga Peninsula, NW Anatolia, derived from a comprehensive set of U-Pb zircon age data obtained from the Eocene to Lower Miocene volcanic units in the region. The timing of extension, granitic magmatism and volcanic activity of the Biga region are then compared and correlated with the northwesterly located Rhodope and Thrace and the easterly located Armutlu-Almacık-Nallıhan regions. The compiled radiometric age data show that calc-alkaline volcanic activity occurred at ~43-15 Ma in the Biga Peninsula, ~43-17 Ma in the Rhodope and Thrace regions, and ~53-38 Ma in the Armutlu-Almacık-Nallıhan region. We discuss the possible cause for the distinct Cenozoic geodynamic evolution of the eastern and western parts of the region, and propose that the Rhodope, Thrace and Biga regions in the north Aegean share the same Late Mesozoic to Cenozoic geodynamic evolution, which is consistent with continuous subduction, crustal accretion, southwestward trench migration and accompanying extension; all preceded by the Late Cretaceous – Paleocene collision along the Vardar suture zone. In contrast, the Armutlu-Almacık-Nallıhan region that lies to the east was shaped by slab break-off and related processes following the Late Cretaceous – Paleocene collision along the İzmir-Ankara suture zone. The eastern and western parts of the region are presently separated by a northeast-southwest trending transfer zone that was likely originally present as a transform fault in the subducted Tethys oceanic crust, and demonstrates that the regional geodynamic evolution can be strongly influenced by the geographical distribution of geologic features on the subducting plate.

Keywords: Aegean; subduction; crustal accretion; slab break-off; transfer zone

1. Introduction

The northern Aegean region, including Rhodope, Thrace and the Biga peninsula of NW Anatolia is a part of the Alpine orogenic belt, and was shaped by subduction, obduction, collision, and post-collisional extension processes during consumption of Tethys oceans. The region is characterized by magmatic associations developed from the Late Cretaceous to Miocene. The Late Cretaceous subduction-related magmatic activity developed in response to Late Mesozoic northward subduction of the northern branch of the Neotethys including the Vardar basin and its eastern continuation in the İzmir-Ankara basins (Şengör and Yılmaz, 1981 and references therein). The subsequent Cenozoic magmatism in the region is regarded as "post-collisional" with respect to the closure of this ocean and collision between the main continental blocks (e.g., Yılmaz et al., 2001). This phase of magmatic activity produced basaltic to rhyolitic volcanism with mainly medium- to high-K calc-alkaline, shoshonitic and locally ultrapotassic associations that were followed by Na-alkaline intra-plate-like basaltic eruptions in the whole region (see Ersoy and Palmer, 2013 and references therein). The geochemical features of the calc-alkaline to ultrapotassic magmatic rocks are interpreted to indicate derivation from mantle sources that had been modified by the previous subduction events, i.e., they are "orogenic" in character. In the literature, the main geodynamic processes proposed to account for this magmatic phase includes; (a) subduction and following roll-back, (b) post-collisional extension with or without trench roll-back, (c) slab break-off, and (d) delamination (Fytikas et al., 1984; Genç, 1998; Aldanmaz et al., 2000; Yılmaz et al., 2001; Marchev et al., 2004; 2010; 2013; Altunkaynak and Genç, 2008; Karacık et al., 2008; Kürkçüoğlu et al., 2008; Georgiev et al., 2009; Okay and Satır, 2000b; Altunkaynak et al., 2012a, 2012b; Bonev et al 2013; Akal, 2013; Gülmez et al., 2013; Ersoy and Palmer, 2013; Ersoy et al., 2014; Kasapoğlu et al., 2016). However, which one(s) of these processes were mainly responsible in shaping the geodynamic history of the region is still debated. On the

basis of mantle tomographic images, that reveal the presence of a single subducting slab beneath the west Aegean region, recent studies have proposed that the Hellenides and the Anatolide-Taurides were accreted to the Eurasian southern active margin (Rhodope-Pontide fragment) by continuous subduction of a single slab since at least the Late Cretaceous (e.g., Jolivet and Brun, 2010). This hypothesis is problematic in the Anatolian area of this region, however, because there ~~are strong evidences~~ for slab break-off processes~~, where it has been interpreted to contain~~ evidence of accretion of tectonic units attributed to several distinct subduction events of the oceanic branches of Neotethys (e.g., Pourteau et al., 2013).

Three regions in the northern Aegean, the Rhodope-Thrace, Biga Peninsula and Armutlu-Almacık-Nallıhan (the Central Sakarya), are characterized by extensive post-collisional magmatic associations developed from the Eocene to Miocene. In the Biga Peninsula, the Middle Eocene to Middle Miocene calc-alkaline to shoshonitic magmatic rocks (e.g., Aldanmaz et al., 2000; Yılmaz et al, 2001; Altunkaynak and Genç, 2008) show ~~great~~ geochemical and geochronological similarities to those of the Rhodope and Thrace regions (e.g., Yılmaz and Polat, 1998; Christofides et al., 2004; Marchev et al., 2004; 2010; Ersoy et al., 2014), while the Armutlu-Almacık-Nallıhan region, that lies to the east of the Biga Peninsula, contains mildly Na-alkaline, low-K (tholeiitic) to middle-K calc-alkaline magmatic rocks, but are ~10 Myr older (Kürkçüoğlu et al., 2008; Gülmez et al., 2013; Kasapoğlu et al., 2016).

We suggest that comparison of the Cenozoic magmatic events of these three regions may ~~give us some clues to expore~~ the Late Mesozoic to Cenozoic tectonic evolution of the Aegean. With this aim, in this study, we present an improved Cenozoic stratigraphy of the Biga Peninsula derived from a new comprehensive set of U-Pb zircon age data obtained from the Eocene to Miocene volcanic units in the region. We also compiled a large dataset of radiometric ages obtained from the magmatic series, and from the metamorphic rocks which

were synchronously deformed under the extensional tectonic regime that extends from Rhodope to western Anatolia. These data have been used to carry out a regional comparison of the magmatic associations of the Biga Peninsula with those of the westerly located Rhodope region and the easterly located Armutlu-Almacık-Nallıhan (Central Sakarya) region. The results are also used to propose a new tectonic scenario involving Mesozoic - Cenozoic geodynamic evolution of the Aegean region.

2. Regional Geology

Basement of the north Aegean region is made up of Eurasia- and Gondwana-derived continental fragments and intervening oceanic units (Figure 1). The continental blocks with Eurasian affinity form the Rhodope-Pontide fragment and include the Rhodope and Strandja massifs in the west, and the İstanbul and Sakarya zones in the east, with the latter being separated by the Intra-Pontide suture. The Rhodope-Pontide fragment is separated from the southerly located Gondwana-derived Hellenides and Anatolide-Taurides along the Vardar and İzmir-Ankara suture zones. The geological features of the north Aegean region (Figure 1) can be divided into three sub-regions: (1) the Rhodope and Thrace region to the west, (2) the Biga Peninsula and (3) the Armutlu-Almacık-Nallıhan region to the east.

2.1. Rhodope and Thrace Region

The pre-Cenozoic basement rocks of the Rhodope to Thrace region, from north to south, is made up of the Balkanides, the Srednogorie Zone, the Strandja and Rhodope massifs, the Circum-Rhodope Belt and the Vardar Zone (Figure 1). Together, the *Balkanides* and the *Srednogorie zone* represent an Andean-type arc and the north-verging fold-and-thrust belt of the southern Eurasian margin with a continental basement (Boccaletti et al., 1974), along which the Tethys Ocean was consumed by north-dipping subduction. The Strandja Massif links the Rhodope and Balkanides to the Pontides in northern Turkey (Figure 1), and consists

of Paleozoic basement and Lower to Middle Triassic - Middle Jurassic cover (Sunal et al., 2011). The Balkanides and Strandja Massif are cut by magmatic rocks of the Srednogorie arc, which is the eastern part of the Apuseni–Banat–Timok–Srednogorie calc-alkaline magmatic belt. Granitic plutons within the Srednogorie arc yielded 92.1±0.3 to 75.6±1.1 Ma zircon U-Pb and 92.5±3.0 to 62.0±4.0 Ma Ar-Ar and K-Ar ages, indicating that the plutons were intruded and cooled between ~92 and ~62 Ma (e.g., Kamenov et al., 2000; von Quadt et al., 2005; Peytcheva et al., 2008; Georgiev et al., 2012) (Figure 2). Similarly, the volcanic products of the arc yielded 94.7±0.4 to 78.9±0.3 Ma zircon U-Pb ages (e.g., Rieser et al., 2008; Marchev et al., 2009; Georgiev et al., 2012). The eastern continuity of this belt is known as Pontide magmatic arc in Turkey (e.g., Şengör and Yılmaz, 1981).

The *Rhodope Massif* is separated from the northerly located Srednogorie zone by the dextral Maritza strike-slip shear zone, which is interpreted as a crustal-scale transpressional shear zone (e.g., Burg et al., 1996). According to Naydenov et al. (2013) the ductile shearing along the Maritza shear zone occurred between 130 and 82-78 Ma, with the younger ages being related to late-stage intrusions within the Srednogorie zone. The Rhodope Massif represents a south-vergent Mesozoic nappe stack progressively grown on a north-dipping subduction front (e.g., Ricou et al., 1998). Several stratigraphic schemes have been proposed for the Rhodope Massif (e.g., Burg et al., 1996; Ricou et al., 1998; Bonev et al., 2006; Jahn-Awe et al., 2012). Overall, it is composed of lower (also known as the Drama nappe) and upper terranes separated by intermediate thrust sheets with both continental and oceanic units (Burg et al., 1996; Ricou et al., 1998). The lower and upper terrains, along with the imbricate unit, were amalgamated by the latest Jurassic to Early Cretaceous (Ricou et al., 1998). The Rhodope Massif experienced high- to ultra-high pressure metamorphism, which yielded three groups of Jurassic-Early Cretaceous, Late Cretaceous and Eocene ages (Wawrzenitz and Mposkos, 1997; Mposkos and Kostopoulos, 2001; Liati et al., 2002).

147 The *Circum-Rhodope Belt* includes low-grade metamorphic rocks that tectonically overly the
148 Rhodope Massif (Figure 1). Further southwest, the Rhodope Massif is separated from the
149 Pelagonian Zone by the Vardar Zone, which is the main suture zone of the Hellenides (see
150 Zachariadis, 2007 and references therein). The Vardar zone contains ophiolite slivers mainly
151 obducted during Jurassic times, and was formed during the Late Cretaceous. The Pelagonian
152 Zone and its Eocene-Miocene HP metamorphic equivalents, the Cyclades (e.g., Ring and
153 Layer, 2003), lie further southwest (Figure 1).

154 Since, at least, the Eocene, the nappe package forming the Rhodope Massif has undergone
155 tectonic extension in association with migmatisation and magmatism (Dinter, 1998; Kilias et
156 al., 1999; Lips et al., 2000; Bonev et al., 2006; Brun and Sokoutis, 2012). Extensional
157 deformation of the Rhodopes, with a top-to-southwest sense of shear, produced several
158 extensional metamorphic complexes, including the Central Rhodope, the Kesebir-Kardamos,
159 and Byala-Reka Kechros domes, and the South Rhodope Core Complex (Figure 1; Lips et al.,
160 2000; Bonev et al., 2013). Radiometric age data from the first three domes, which are located
161 to the north-northeast, indicate an early to late Eocene exhumation and cooling history (e.g.,
162 Dinter, 1998; Lips et al., 2000; Peytcheva et al., 2004; Bonev et al., 2006, 2013).
163 Extensionally deformed rocks of the South Rhodope Core Complex, yield mainly Oligocene-
164 Miocene cooling ages (e.g., Wawrzenitz and Krohe, 1998; Lips et al., 2000). Extensional
165 deformation in the Rhodopes was accompanied by intense magmatic activity producing syn-
166 to post-extensional granitoids with ~55 to 20 Ma intrusion ages, calc-alkaline (CA) to
167 shoshonitic/ultrapotassic (SHO-UK) volcanic rocks with ~43 to 26 Ma ages, and Na-alkaline,
168 Na-alkaline OIB-like intra-plate basalts with ~28-26 Ma ages (Figure 2; Singer and Marchev,
169 2000; Marchev et al., 2004; 2010; Christofides et al., 2004).

170 The metamorphic rocks of the Rhodope Massif and the Strandja zone are covered by the
171 Eocene to Pliocene sedimentary rocks of the Thrace Basin, which is the largest sedimentary

basin in the region (Figure 1; Siyako and Huvaz, 2007; Elmas, 2012; Kilias et al., 2013). Thrace basin, with its triangular shape, contains sedimentary infill up to ~9 km thick (e.g., Elmas, 2012 and references therein). The sedimentary succession of the Thrace basin includes CA to SHO-UK volcanic intercalations with Oligocene – Early Miocene ages (Ercan et al., 1995; 1998; Christofides et al., 2004; Ersoy et al., 2014). Na-alkaline basalts of ~15-5 Ma also occur in Turkish part of the basin (Figure 2; Ercan et al., 1998; Aldanmaz et al., 2006).

2.2. Biga Peninsula

The stratigraphy of the Biga Peninsula, located south of the Thrace basin (Figure 1), comprises; (1) metamorphic rocks of the Ezine Group and (2) metamorphic/non-metamorphic rocks of the Sakarya Zone, which are separated by (3) ophiolitic Çetmi mélange, and (4) Eocene to Upper Miocene volcano-plutonic complex and sedimentary rocks (Okay et al., 1991; Beccaletto et al., 2007; Figure 3).

The Ezine Group is composed of schists, marbles and amphibolites with eclogitic relics, which were dated at 69-65 Ma (Okay and Satır, 2000a). The Çetmi mélange includes several slices/blocks including eclogites (with 100.3±2.8 Ma Rb-Sr age; Okay and Satır, 2000b) embedded in a late Early Cretaceous greywacke–shale matrix (Beccaletto et al., 2005). On the basis of the lithology and age determinations, Beccaletto et al. (2005) correlated this unit with the mélange-like units in the Rhodope Massif. The Sakarya Zone consists of (1) the gneisses, amphibolites, marbles, high-grade schists, and meta-ophiolites of the Kazdağ Massif (Duru et al, 2004; Erdoğan et al., 2013 and references therein) and (2) the Karakaya Complex, with a common cover of Jurassic-Cretaceous sedimentary rocks. The Karakaya Complex is made up of; (a) Permian-Triassic oceanic assemblages and Late Triassic HP rocks, and (b) strongly deformed and relatively non-metamorphic sedimentary and volcano-sedimentary units (Okay and Göncüoğlu, 2004 and references therein).

Similarly to the Rhodope region, the Biga Peninsula underwent a regional extension since the earliest Eocene, at least. The metamorphic rocks are characterized by ductile-to-brittle deformation structures, which are consistent with a regional NE–SW-oriented extension (Beccaletto et al., 2007; Aygül et al, 2012). The undeformed Karabiga pluton, with a 52.7±1.9 U-Pb zircon age, intrudes the Kemer metamorphics (Figure 3; Beccaletto et al., 2007). The metamorphic rocks of the Kazdağ Massif were also extensionally exhumed along the Şelale and Alakeçi detachment faults during the Late Oligocene – Early Miocene (Cavazza et al., 2009; Okay and Satır, 2000b). The Evciler pluton with ~28 Ma intrusion (amphibole Ar/Ar) and 28-20 Ma cooling (biotite Ar/Ar and Rb-Sr) ages (Delaloye and Bingöl, 2000; Okay and Satır, 2000b; Altunkaynak et al., 2012a) was emplaced coeval with the exhumation of the Kazdağ Massif. In addition to the extension-related plutons, the İlyasdağ meta-granitoid in Marmara Island was associated with northward thrust sheeting and yielded a 47.6±2 Ma intrusion (U-Pb zircon) age (Ustaömer et al., 2009). Dextral strike-slip shearing in the Kapıdağ peninsula was also associated with intrusion of the northern Kapıdağ pluton, which yielded ~45-38 Ma intrusion (K-Ar amphibole) and ~45-38 Ma cooling (biotite K-Ar) ages (Delaloye and Bingöl, 2000; Altunkaynak et al., 2012a; Türkoğlu et al., 2016). The other plutons in the Biga Peninsula are generally Oligocene – Miocene in age (with 28-23 Ma intrusion ages) which are widely exposed in the southeast part of the peninsula (Delaloye and Bingöl, 2000; Karacık et al., 2008; Altunkaynak et al., 2012b; Aysal, 2015). The pre-Cenozoic basement rocks of the Biga Peninsula are covered by the Paleogene-Neogene units that comprise mainly volcanic rocks and more scarce sedimentary units.

2.3. Armutlu-Almacık-Nallıhan (Central Sakarya) region

The pre-Cenozoic basement of the region along the Armutlu Peninsula to Almacık Mountains and Nallıhan is characterized by; (1) the Palaeozoic sedimentary rocks of the İstanbul Zone, (2) the Sakarya Zone, (3) the rocks of the Intra-Pontide zone as a mixture of (1) and (2), (4)

ophiolite and mélange rocks of both the İzmir-Ankara and Intra-Pontide suture zones, and (5) high-pressure (HP) metamorphic rocks of the Tavşanlı Zone of the Anatolides (Figures 1 and 4). The İstanbul Zone is separated from the Sakarya zone along the Intra-Pontide suture (Robertson and Ustaömer, 2004), which is overprinted today by segments of the dextral North Anatolian Fault system (Figure 4). Akbayram et al., (2013) provided 158–111 Ma (Late Jurassic–Early Cretaceous) Rb–Sr mica and Sm–Nd garnet ages from the metamorphic rocks that date the amalgamation of the Sakarya and İstanbul zones.

The Sakarya zone in this region is made up of a Variscan basement, Permo-Triassic Karakaya Complex and Liassic to Lower Cretaceous non-metamorphic sedimentary cover. The Uludağ Massif is made up of gneiss and marble with ~49 and 36-30 Ma cooling ages, and represents an Oligocene ductile strike-slip shear zone which was active between 38-27 Ma (Okay et al., 2008).

In the southern parts of this area, between Bilecik and Nallıhan (known as the Central Sakarya Basin), the Upper Jurassic - Lower Cretaceous limestones are overlain by the Upper Cretaceous flysch-type sediments and then by the Paleocene reef limestones (Kasapoğlu et al., 2016). To the north, these formations pass into deep sea turbidites with pyroclastic intercalations (Figure 5) (Özcan et al., 2012). The Upper Cretaceous – Paleocene sedimentary units are overlain by the terrestrial sediments, which contain basaltic to rhyolitic Eocene volcanic rocks of Kızderbent volcanics (~53–38 Ma) in the north and the Nallıhan volcanics (~52–47 Ma) in the south (Genç and Yılmaz, 1997; Kürkçüoğlu et al., 2008; Gülmez et al., 2013; Kasapoğlu et al., 2016).

Ophiolitic rocks occur within the İzmir-Ankara zone as south-verging tectonic slices between the Sakarya zone of the Pontides and the Tavşanlı zone of the Anatolides (Figure 4). The metamorphic sole rocks of these bodies yield ~100-90 Ma Ar-Ar amphibole ages that represent the initial stage of intra-oceanic subduction along the Neo-Tethys (e.g., Önen, 2003

and references therein). The ophiolite and ophiolitic mélange rocks of the İzmir-Ankara suture zone are tectonically underlain by the HP micaschist-marble sequence of the Tavşanlı Zone, which represents the subducted passive northernmost margin of the Anatolide-Tauride Block (Okay et al., 2001). Recently, Fornash et al. (2016) presented; (a) 93-90 Ma Ar/Ar phengite ages from the lawsonite eclogite and (b) 82±2 Ma Ar/Ar phengite ages from the retrogressed, epidote-eclogite from an eclogite-bearing slice, which are interpreted as the age of peak and retrograde metamorphism, respectively. All the pre-Cenozoic rock units in this region, especially those of the Tavşanlı Zone, are cut by undeformed Eocene granitoids with intrusion ages of ~53 – 46 Ma (e.g., Altunkaynak et al., 2012a).

3. Eocene-Miocene Volcano-Sedimentary Stratigraphy of the Biga Peninsula

The pre-Cenozoic basement rocks of the Biga Peninsula are covered by Paleogene-Neogene volcanic and sedimentary units, which are essentially the southward continuation of the Thrace Basin and of the sedimentary succession in the Gelibolu Peninsula (Figure 3). Volcanic intercalations are scarce in the Thrace Basin, whereas the Cenozoic cover in the Biga Peninsula is characterized by the widespread volcanic rocks (e.g., Ercan et al., 1995; 1998; Elmas, 2012; Ilgar et al., 2012).

In the Biga Peninsula, the Eocene sedimentary series begin with the conglomerates of the Fıçıtepe formation, which are interpreted as braided fluvial and flood plain deposits (Elmas et al., 2016; Ilgar et al., 2012). On the basis of fossil associations, Ilgar et al. (2012) suggested a middle Eocene age. The Fıçıtepe Formation is transitionally overlain by the shallow marine limestones of the Soğucak Formation in the Gelibolu Peninsula that lies to the north (Elmas, 2012), but in the Biga Peninsula the Soğucak Formation has very limited outcrops. The Soğucak Formation in the Gelibolu Peninsula is transitionally overlain by the marl, sandstone, shale and tuff alternation of the Ceylan Formation (Elmas, 2012). The Ceylan Formation is made up of sandstone-claystone alternations and greenish tuff intercalations in the Biga

Peninsula (Elmas et al., 2016). Ilgar et al. (2012) suggested that the Ceylan Formation is Late Eocene in age. The Fıçıtepe, Soğucak and Ceylan formations alternate with several volcanic units, from which ~43-34 ages are reported (e.g., Ercan et al., 1995).

Oligocene sedimentary units of the Thrace Basin and Gelibolu Peninsula have not been reported on the Biga Peninsula. Instead, the Oligocene is represented by widespread volcanic and plutonic rocks (Figure 3). Higher in the stratigraphic section there are Miocene coal-bearing fluvial to lacustrine sediments (such as Küçükkuyu, Çan and Soma formations; Ilgar et al., [2012] and references therein), that are interfingered with widespread volcanic rocks which are generally located to the south of the region (Figure 3).

The volcanic stratigraphy of the Eocene-Oligocene volcanic rocks in the Biga region is difficult to establish, because the region is heavily forested and the Cenozoic volcanic rocks are widely affected by hydrothermal alteration. In order to address this problem, we collected a large set of volcanic rocks from both fresh and highly altered outcrops, from which we selected 24 samples for dating from rock units in which the stratigraphy was previously ambiguous. Our data were then combined with age data from previous radiometric studies to produce a revised volcano-stratigraphy of the Biga Peninsula. A large number of local unit names have been included in recently presented stratigraphic sections (e.g., Dönmez et al., 2005), so these have been simplified by combining them as members of a single unit. We have also preferred to use the early-suggested unit names (e.g., Balıklıçeşme and Kirazlı volcanics of Ercan et al., [1995], Hallaçlar volcanics of Krushensky [1976]). Because this study has concentrated on the Eocene-Oligocene volcanic rocks, the Lower-Middle Miocene volcanic units around Ezine, Ayvacık and Gülpınar (Figure 3) are collectively grouped as the Ezine-Ayvacık volcanics. The other units identified here are the Lower Miocene Dedetepe volcanics and the Upper Miocene Taştepe volcanics.

In the Biga Peninsula, the volcanic rocks emplaced between ~43 and ~36 Ma (upper Lutetian – lower Priabonian) are grouped under the name of Balıklıçeşme volcanics which term was first used by Ercan et al. (1995) for the Eocene volcanic rocks around Biga. The Balıklıçeşme volcanics consists of various members, which were previously assigned as separate units by Dönmez et al., (2005) and Genç et al. (2012). The Kirazlı volcanics include andesitic to rhyolitic rocks of several members. The rhyolitic rocks cropping out around the Dededağ volcanic centre were previously correlated with the marine ignimbrites in the Ceylan Formation, and hence, were assigned as Eocene (Dönmez et al., 2005; Genç et al. 2012). However, the new age data indicates that the rhyolitic volcanics are Oligocene in age, and therefore are included as a member in the Kirazlı volcanics. The Hallaçlar volcanics, described first by Krushensky (1976), are composed of andesitic to dacitic volcanic associations located between Havran and Gönen towns (Figure 3). The Miocene andesitic to rhyolitic rocks overlying the Hallaçlar Formation around Yenice are known as Dedetepe volcanics (Krushensky, 1976) (Figure 3). The details of the Lower-Middle Miocene andesitic to rhyolitic volcanic units of the Ezine and Ayvacık volcanics are given by Genç (1998), Akal (2013) and Aldanmaz et al. (2000). In the Biga Peninsula, the last phase of magmatic activity is represented by the Late Miocene Taştepe basalts emplaced around Ezine (Aldanmaz et al., 2000; Figure 3). Overall, therefore, the volcanic units of the Biga Peninsula comprise; (1) the upper Lutetian – lower Priabonian Balıklıçeşme volcanics, (2) the Oligocene Kirazlı volcanics, (3) the Upper Oligocene Hallaçlar volcanics, (4) the Lower Miocene Dedetepe volcanics, (5) the Lower – Middle Miocene Ezine-Ayvacık volcanics, and (6) the Upper Miocene Taştepe volcanics (Figures 3 and 9).

4. Zircon Geochronology

In this study, eight samples from the Balıklıçeşme volcanics, ten samples from the Kirazlı volcanics, five samples from the Hallaçlar volcanics and one sample from the Dedetepe

volcanics were collected for dating by the U-Pb zircon method. The locations, stratigraphic positions, petrographic features, zircon characteristics and the obtained ages are summarized in Table 1.

Zircons were separated in the sample preparation laboratory at the Geological Engineering Department of Dokuz Eylül University from 15-20 kg samples using standard mineral separation techniques. The rocks were crushed to coarse sand size with a tungsten carbide jaw crusher. Subsequently, zircons were concentrated by flotation on a shaking table, sieving, magnetic separation and heavy liquids. A representative batch of 60 zircon crystals with grain sizes of 150 - 300 µm was manually picked and mounted in Araldite 2020 resin. After polishing, cathodoluminescence (CL) images were taken using a CL detector connected to a Jeol JX A-8900RL electron microprobe at the Institute for Geosciences, University of Mainz. U, Th and Pb isotopes were measured by LA-ICP-MS (Institute for Geosciences, University of Mainz) using an Agilent 7500ce quadrupole ICP-MS system coupled to an ESINWR193 ArF excimer laser system with a 193 nm output wavelength. The laser system is equipped with a two volume sample chamber (10 cm × 10 cm). After pre-ablation, analyses were conducted using a spot size of 30 µm, 20 s warm up time, 30 s dwell time and 20 s washout time. The repetition rate was 10 Hz at pulse energy of 3.5 Jcm^{-2}. The instrument was tuned for maximum sensitivity at low oxide formation rates of <0.5 %. The dwell times for individual masses are 10 ms for masses 232 and 238, and 30 ms for 202, 204 and 208. Dwell times of 40 and 60 ms were used for masses 206 and 207, respectively. For a first step data reduction, the time-resolved signal was processed using the program GLITTER 4.4.1 (www.glitter-gemoc.com, Macquarie University, Sydney, Australia). Time-dependent laser and mass spectrometer induced inter-element fractionation (Pb/U), mass fractionation, as well as common lead, were corrected afterwards using an Excel spreadsheet of ComPbcorr#318 (Andersen, 2002). The inter-element fractionation during ablation was corrected linearly. For

this purpose, ablation conditions such as spot sizes and ablation times were kept constant during each session. The interference of ^{204}Hg on ^{204}Pb was corrected by measuring ^{202}Hg and calculating ^{204}Hg using the natural ^{204}Hg/^{202}Hg ratio of 0.2299. Ages, uncertainties and concordia diagrams were produced using Isoplot3 for Excel (Ludwig, 2003). Concordia ages are plotted with 2σ uncertainty ellipses and discordia intercept ages are given at 95% confidence (Supplementary Material 2). Analyses were calibrated using a GJ-1 (GEMOC) zircon (Slama et al., 2008). Reproducibility and accuracy were controlled by repeated analyses of Plesovice and 91500 reference zircons, from Jackson et al. (2004) and Wiedenbeck et al. (1995), respectively, treated as unknown samples; measured values deviate <2% from the published values.

6. Discussion

In this section, the geochronology of the magmatic rocks of the Biga Peninsula will be compared and correlated with those of; (a) the Rhodope and Thrace region in the west and (b) the Armutlu-Almacık-Nallıhan region in the east. We propose that the differences and similarities between the Cenozoic magmatic events and volcanic stratigraphy of these regions were related to their distinct geodynamic evolution since, at least, Late Cretaceous. Hence, the Eocene to Miocene tectono-magmatic events of these regions will then be discussed in terms of the Late Cretaceous to Miocene regional geodynamic events in the wider Aegean region.

6.1. Correlation and Comparison of the Eocene-Miocene Magmatic Events

In this study, the Eocene to Miocene volcanic rock units in the Biga Peninsula yielded U-Pb zircon ages ranging from 43.15 to 22.47 Ma. The Balıklıçeşme volcanics were emplaced between ~43-35 Ma (Middle-Late Eocene), the Kirazlı volcanics between ~33-25 Ma (Early-Late Oligocene), and the Hallaçlar volcanics between 28-23 Ma (Late Oligocene). These units are overlain by the Ezine-Ayvacık and Dedetepe volcanics of ~22-15 Ma (Early-Middle

Miocene). All these units are composed of calc-alkaline to shoshonitic series volcanics with subduction-related geochemical features (i.e., orogenic) (e.g., Ercan et al., 1998; Aldanmaz et al., 2000; Altunkaynak and Genç, 2008; Genç et al., 2012; Akal, 2013) and with their emplacements being restricted to the ~43–15 Ma interval. These are followed by the eruption of the Na-alkaline, OIB-type Taştepe basalts between 11.0 to 8.3 Ma (Late Miocene). These age data indicate that the orogenic volcanic activity in the Biga Peninsula was continued almost without interruption from the Middle Eocene (Lutetian) to the Middle Miocene (Figures 9 and 10a).

To the NW of the Biga Peninsula, throughout the Rhodope Massif and the Thrace Basin, the Cenozoic orogenic volcanic rocks yield ~43 to 17 Ma ages that completely overlap those of the Biga Peninsula (Figure 10a). Furthermore, two pulses of Na-alkaline intraplate basaltic volcanism developed at ~28-26 Ma in the Rhodope Massif and 15-8 Ma in the Thrace Basin (Marchev et al., 2004; Ersoy et al., 2014).

Along the northern part of the Biga peninsula (the southern Marmara), Eocene plutons with 52 to 37 Ma intrusion ages are exposed (Figures 3 and 10a). Among these, the undeformed Karabiga pluton intruded into the extensionally deformed Kemer micaschist at ~52 Ma (Beccaletto et al., 2007). However, the northern Kapıdağ pluton with a 48-42 Ma intrusion age is associated with the NW-SE-trending strike-slip shear zone (Kapıdağ shear zone; Türkoğlu et al., 2016; Figure 3). Synchronously with this activity, the İlyasdağ meta-granitoid with a ~48 Ma intrusion age is also associated with northward thrusting of several units of high-grade rocks (Ustaömer et al., 2009). The other granitoid plutons of the Biga Peninsula generally yield Oligocene to Miocene intrusion ages (~28 to 22 Ma; Figures 9 and 10a). Overall, therefore, granitoid magmatism in the Biga Peninsula developed between ~52 and 22 Ma. In the Rhodope region, the cooling age data from the metamorphic rocks exhumed along the detachment faults coincide ~~well~~ with those obtained from the granitoid intrusions (Figure

10a) (Dinter, 1998; Wawrzenitz and Krohe, 1998; Kilias et al., 1999; Lips et al., 2000; Peytcheva et al., 2004; Bonev et al., 2006, 2013). In this case, the granitoid magmatism in both the Biga and Rhodope regions ~~were~~ synchronously related to extensional tectonics. Exceptionally, the data from the syn-kinematic İlyasdağ meta-granitoid and the northern Kapıdağ pluton indicate that they were emplaced along a transpressional field. Therefore, the extensional tectonics in the Biga Peninsula was also coeval with local transpressional regime (Kapıdağ shear) along the SW continuation of the Maritza fault.

Overall, the geochronological data and the regional distribution of magmatic rocks in the Biga Peninsula and the Rhodope-Thrace regions reveal that both regions are characterized by; (1) extensive "orogenic" volcanic activity developed between ~43-15 Ma with decreasing ages from north-northeast to south-southwest (see Figures 2 and 10a), and (2) syn-extensional granitoid magmatism that commenced in the earliest Eocene. Hence, these data suggest that the Biga Peninsula and the Rhodope-Thrace region share the same Eocene to Miocene tectono-magmatic evolution that is characterized by post-collisional extension. Considering the mantle tomographic images (e.g., Jolivet and Brun, 2010) and the southward migration of deformation and magmatic activity, the extensional tectonics in this region can be attributed to southward-migration of the Aegean subduction zone (see also Jolivet and Brun, 2010; van Hinsbergen et al., 2005; Brun and Sokoutis, 2012).

However, the Eocene volcanic rocks of the Armutlu-Almacık-Nallıhan region show some distinctions from the Biga and Rhodope regions; (1) except for the Miocene volcanism of the Galatean and Afyon-Isparta regions, and local Miocene basaltic extrusions (see Gülmez et al. 2013; Figure 10), the volcanic activity here is restricted to 53-38 Ma in the north and 52-47 Ma in the south (see Figures 2, 4, 5 and 10), (2) the Eocene volcanism did not migrate southward, (3) the volcanic (and plutonic) rocks display pronounced alignments along E-W-trending narrow zones (Figure 2), and (4) the geochemical features of the Eocene volcanics

reflects the effects of an asthenospheric source (with sodic alkaline character) in the southern region, with all of these features being attributed to slab-break-off processes (see Gülmez et al., 2013; Kasapoğlu et al., 2016).

6.2. Regional Geodynamic Implications for the Aegean

In this section, we construct a Late Cretaceous to Miocene geodynamic model for the evolution of the Aegean region that includes the Rhodope-Thrace-Biga area in the west and Armutlu-Almacık-Nallıhan area in the east (Figures 1 and 11). The model illustrated in Figure 11, combines our age data with the histories of the consumption of oceanic branch(es) of the Tethys, the tectonic settings of the magmatic units, the tectonic significance of the Bornova Flysh zone (Okay et al., 2012) and the metamorphic evolution of the continental units.

Following the latest Jurassic–Early Cretaceous amalgamation of the Rhodopes and Balkanides in the west (e.g., Bonev et al., 2006; Ricou et al.1998) and the Early Cretaceous closure of the Intra-Pontide ocean in the east (e.g., Akbayram et al., 2013), a magmatic arc, the Srednogorie - Pontide arc, developed in response to the Late Cretaceous subduction of the Vardar – İzmir-Ankara oceans (e.g., Georgiev et al., 2012; Gülmez et al., 2016) (Figure 11). Intra-oceanic subduction at ~100-90 Ma (e.g., Önen, 2003) preceded the Pontide magmatic activity of ~92-70 Ma, while the Srednogorie was probably Andean-type (e.g., Gallhofer et al., 2015). These distinct settings ~~might~~ be accommodated by a transform fault zone, as illustrated on Figure 11a.

As proposed by Naydenov et al. (2013), Late Cretaceous amalgamation of a micro-continent along the Rhodopes may have led to ~N–S compression, which then resulted in dextral shearing along the Maritza shear zone (MSZ) and related granitoid emplacement at 82-78 Ma (Figure 11b). However, the Late Cretaceous - Early Paleogene evolution in the east displays some differences. During this interval, ophiolite obduction onto the Anatolide - Tauride block

443 was followed by deep subduction of the northern edge of this platform, giving rise to HP
444 metamorphism of the Tavşanlı Zone at ~90-80 Ma (Pourteau et al., 2016 and references
445 therein). The tectonic position and deposition age of the Bornova flysch zone are of particular
446 interest regarding the distinct geodynamic evolutions of the eastern and western Aegean
447 domains because it is believed to have been deposited along a strike-slip transfer zone at the
448 western margin of the Taurides during the Latest Cretaceous to Danian (Okay et al., 2012),
449 coeval with the HP metamorphism of the Tavşanlı Zone.

450 During the Latest Cretaceous to Paleocene times, the oceanic lithosphere of the Vardar and
451 İzmir-Ankara ocean(s) was completely consumed (see Okay et al., 2001 and Zachariadis,
452 2007 and references therein). It is important to note that this time is one of the most critical
453 periods in the geodynamic history of the region, and holds a key in understanding the distinct
454 evolution of the both sides. While, the subduction along the Vardar Ocean migrated towards
455 the southwest by accretion of the overlying continental blocks (i.e., Pelagonian zone) via
456 mantle-crust decoupling on a single subducting plate (see van Hinsbergen et al., 2005 and
457 Jolivet and Brun, 2010), the subducted oceanic lithosphere of the İzmir-Ankara ocean broke-
458 off and gave rise to exhumation of the Tavşanlı Zone (e.g., Okay et al., 2001) (Figure 11c).
459 The Afyon zone then underwent HP metamorphism during the latest Cretaceous as a result of
460 internal imbrications of the Anatolide-Tauride platform (Candan et al., 2005).

461 During the Early Eocene, the crustal accretion and southward migration on the single
462 subduction zone in the west created back-arc extension across the Rhodope – Thrace – Biga
463 region (e.g., Jolivet and Brun, 2010; van Hinsbergen et al., 2005; Brun and Sokoutis, 2012;
464 Figure 11d). During this time, syn-extensional plutons of Rhodope were emplaced in the
465 footwalls of the detachment faults (Bonev et al., 2016; 2013; Dinter, 1998; Peytcheva et al.,
466 2004), and the Thrace basin ~~is~~ developed. In addition, strike-slip shearing along the Maritza
467 fault likely migrated further southeast, as evidenced by the 48-42 Ma Kapıdağ shear zone

(KSZ) (Türkoğlu et al., 2016) due to local compression in the region, as a consequence of ongoing continental contraction between the Pontides and the Anatolide-Taurides.

Breaking-off of the subducted slab of the İzmir-Ankara ocean in the east caused asthenospheric upwelling and mafic magmatism at ~53-47 Ma along the Armutlu-Almacık - Nallıhan region (Gülmez et al., 2013; Kasapoğlu et al., 2016), with the western boundary marked by the transfer fault zone (Figure 11d). The Eocene HP metamorphism of the Cyclades has been attributed to closure of the Pindos Ocean (e.g., Ring and Layer, 2003) is also reported in the westernmost Menderes Massif (Candan et al., 1997), revealing that Pindos ocean continued to the east in western Anatolia (Figure 11d). During the Middle to Late Eocene, the Menderes Massif was buried and underwent Barrovian metamorphism (~43-35 Ma; Schmidt et al., 2015) (Figure 11e).

Southwestward migration of the subduction in the west of the area led to an increase in the degree of extensional tectonics in the Rhodope-Thrace (and Biga) regions (e.g., Brun and Sokoutis, 2012). As a consequence, extensive "orogenic" volcanic activity and syn-extensional plutons developed during the Middle Eocene to Late Oligocene (Figure 11e). The clockwise rotation of the western part of the Aegean since 45 Ma (Brun and Sokoutis, 2012) also meant that the magmatism that had been restricted to the Rhodope, Thrace and Biga regions, now migrated southwestward due to the rotational roll-back that continued until the Late Miocene (see Ersoy and Palmer, 2013 for a review). This rotational movement is bordered by the transfer fault that was formed in the Tethys Ocean. During the Miocene to Recent period this fault was reactivated and resulted in strike-slip deformation along the İzmir-Balıkesir transfer zone (Erkül et al., 2005) (see inset map in Figure 2). Accretion of the external Hellenides caused the transfer zone to migrate south during the Oligocene (Figure 11e).

The Oligocene ~N-S compression in the northeast of the region resulted in dextral shearing and granitoid intrusion along the Uludağ shear zone (USZ) (Figure 11e). The dextral offset along the younger North Anatolian Fault zone (NAFZ, Fig. 1) (Yaltırak, 2002) indicates that the compressional deformation and related NW-SE-trending dextral shearing migrated from the northwest to southeast; from Maritza at ~80 Ma to Kapıdağ at ~50 Ma, and eventually to Uludağ shearing at ~27 Ma.

The Aegean region lies in the western part of the Alpine-Himalayan orogenic belt, so that its overall geodynamic evolution is ultimately driven by consumption of the Tethys Ocean and the associated processes of subduction, continental collision, crustal subduction and accretion (see Ersoy and Palmer, 2013 and references therein for a recent review). While this overall pattern is well-characterized, the detailed controls over the geodynamic evolution of individual segments of the orogenic belt are far more varied. Detailed analysis of the ages and styles of volcanism in the Aegean (summarized in Figure 11) reveal that important characteristics of the regional geodynamic evolution were driven by the geographical distribution of features of the Tethys Ocean. In particular, the jumping of the subduction zone in the western part of the region likely resulted from the successive addition of microcontinents (Pelagonia and the External Hellenides) to the Balkanides and Strandja Massif. In addition, the slab break-off in the eastern part of the region was likely strongly influenced by the presence of a pre-existing transfer fault in the Tethys Ocean that led to the separate geodynamic evolution of the eastern and western parts of the region.

6. Conclusions

New zircon U-Pb ages ~~have shown~~ that the Cenozoic calc-alkaline volcanism in the Biga Peninsula, NW Anatolia developed interruptedly between ~43 and 15 Ma. These ages overlap completely with those for similar volcanic products of the Rhodope and Thrace regions further NW. Collectively, the timing and style of volcanic activity of these regions

significantly differ from post-collisional volcanism in the easterly located Armutlu-Almacık and Nallıhan regions, where the Lower Eocene volcanic activity show a clear Na-alkaline signature that is indicative of asthenospheric contributions. Hence, western portion of this area of the Aegean, that includes the Rhodope to Biga region in the west, has a distinct geodynamic history from the Armutlu-Almacık-Nallıhan region in the east. Following the Late Cretaceous – Paleocene collision along the Vardar suture zone, the Rhodope, Thrace and Biga regions in the west experienced a geodynamic regime, involving crustal accretion, southwestward migration of the subduction and related extension processes. In the Armutlu-Almacık-Nallıhan region to the east, however, the geodynamic evolution was shaped by slab break-off and related processes following the Late Cretaceous – Paleocene collision along the İzmir-Ankara suture zone. The western area of the region was rotated clock-wise rolled-back into the present day position by the continued accretion of continental fragments. The distinct geodynamics of the eastern and western domains was initially marked by a transfer fault that was inherited from the Tethys Ocean in the Late Cretaceous, and was subsequently reactivated as crustal transfer zone in the Eocene. These observations suggest that the distribution of geologic features on the subducting plate (the distribution of microcontinents and transfer faults) can play a significant role in continental geodynamic evolution long after the oceanic lithosphere has been subducted.

Acknowledgments

This work supported by the Scientific and Technological Research Council of Turkey (grant number: TUBITAK-CAYDAG-12Y128). Uğur Öven and Bülent Kasapoğlu are thanked for their help during field studies.

References

Akal, C., 2013. Coeval Shoshonitic-Ultrapotassic Dyke Emplacements within the Kestanbol Pluton, Ezine – Biga Peninsula (NW Anatolia). Turkish Journal of Earth Sciences 22, 220-238. doi:10.3906/yer-1202-1

Akbayram, K., Okay, A.I., Satır, M., 2013. Early Cretaceous closure of the Intra-Pontide Ocean in western Pontides (northwestern Turkey). Journal of Geodynamics 65, 38– 55. doi:10.1016/j.jog.2012.05.00

Aldanmaz, E., Köprübaşı, N., Gürer, Ö.F, Kaymakçı, N., Gourgaud, A., 2006. Geochemical constraints on the Cenozoic, OIB-type alkaline volcanic rocks of NW Turkey: Implications for mantle sources and melting processes. Lithos 86, 50–76. doi:10.1016/j.lithos.2005.04.003

Aldanmaz, E., Pearce, J.P., Thirwall, M.F., Mitchell, J.G., 2000. Petrogenetic evolution of late Cenozoic, post-collision volcanism in western Anatolia, Turkey. Journal of Volcanology and Geothermal Research 102, 67–95.

Altunkaynak, Ş., Dilek, Y., Genç, C.Ş., Sunal, G., Gertisser, R., Furnes, H., Foland, K.A., Yang, J., 2012b. Spatial, temporal and geochemical evolution of Oligo–Miocene granitoid magmatism in western Anatolia, Turkey. Gondwana Research 21, 961–986. doi:10.1016/j.gr.2011.10.010

Altunkaynak, Ş., Genç, C.Ş., 2008. Petrogenesis and time-progressive evolution of the Cenozoic continental volcanism in the Biga Peninsula, NW Anatolia (Turkey). Lithos 102, 316–340. doi:10.1016/j.lithos.2007.06.003

Altunkaynak, Ş., Sunal, G., Aldanmaz, E., Genç, C.Ş., Dilek, Y., Furnes, H., Foland, K.A., Yang, J., Yıldız, M., 2012a. Eocene Granitic Magmatism in NW Anatolia (Turkey) revisited: New implications from comparative zircon SHRIMP U–Pb and ^{40}Ar–^{39}Ar geochronology and isotope geochemistry on magma genesis and emplacement. Lithos 155, 289–309. doi:10.1016/j.lithos.2012.09.008

Andersen, T., 2002. Correction of common lead in U–Pb analyses that do not report 204Pb. Chemical Geology 192, 59–79.

568 Aygül, M., Topuz, G., Okay, A.İ., Satır, M., Meyer, H-P., 2012. The Kemer Metamorphic
569 Complex (NW Turkey): A Subducted Continental Margin of the Sakarya Zone. Turkish
570 Journal of Earth Sciences 21, 19–35. doi: 10.1016/j.jseaes.2015.07.005

571 Aysal, N., 2015. Mineral chemistry, crystallization conditions and geodynamic implications
572 of the Oligo–Miocene granitoids in the Biga Peninsula, Northwest Turkey. Journal of Asian
573 Earth Sciences 105, 68–84. doi:10.1016/j.jseaes.2015.03.026

574 Beccaletto, L., Bartolini, A.C., Martini, R., Hochuli, P.A., Kozur, H., 2005. Biostratigraphic
575 data from the Çetmi mélange, northwest Turkey. Palaeogeographic and tectonic implications.
576 Palaeogeography, Palaeoclimatology, Palaeoecology 221, 215–44. doi:
577 10.1016/j.palaeo.2005.02.011

578 Beccaletto, L., Bonev, N., Bosch, D., Bruguier, O., 2007. Record of a Palaeogene syn-
579 collisional extension in the north Aegean region: evidence from the Kemer micaschists (NW
580 Turkey). Geological Magazine 144, 393–400. doi:10.1144/SP291.6

581 Boccaletti, M., Manetti, P., Peccerillo, A., 1974. The Balkanids as an Instance of Back-Arc
582 Thrust Belt: Possible Relation with the Hellenids. Geological Society of America Bulletin 85,
583 1077-1084.

584 Bonev, N., Burg, J.-P., Ivanov, Z., 2006. Mesozoic–Tertiary structural evolution of an
585 extensional gneiss dome—the Kesebir–Kardamos dome, eastern Rhodope (Bulgaria–Greece).
586 International Journal of Earth Science 95, 318–340. doi:10.1007/s00531-005-0025-y

587 Bonev, N., Spikings, R., Moritz, R., Marchev, P., Colligns, D., 2013. $^{40}Ar/^{39}Ar$ age
588 constraints on the timing of Tertiary crustal extension and its temporal relation to ore-forming
589 and magmatic processes in the Eastern Rhodope Massif, Bulgaria. Lithos 180–181, 264–278.
590 doi: /10.1016/j.lithos.2013.05.014

591 Brun J.-P., Sokoutis, D., 2012. 45 m.y. of Aegean crust and mantle flow driven by trench
592 retreat. Geology 38(9), 815–818. doi: 10.1130/G30950.1

593 Burg, J.-P., Ricou, L.-E., Ivanov, Z., Godfriaux, I., Dimov, D., Klain, L. 1996. Syn-
594 metamorphic nappe complex in the Rhodope Massif: structure and kinematics. Terra Nova 8,
595 6–15.

596 Candan, O., Çetinkaplan, M., Oberhänsli, R., Rimmelé, G., Akal, C., 2005. Alpine high-
597 P/low-T metamorphism of the Afyon Zone and implications for the metamorphic evolution of
598 Western Anatolia, Turkey. Lithos 84, 102–124. doi:10.1016/j.lithos.2005.02.005

599 Candan, O., Dora, O.Ö., Oberhänsli, R., Oelsner, F., Durr, S. 1997. Blueschist relics in the
600 Mesozoic cover series of the Menderes Massif and correlations with Samos Island, Cyclades.
601 Schweizerische Mineralogische und Petrographische Mitteilungen 77, 95–99.

602 Cavazza, W., Okay, A.I., Zattin, M., 2009. Rapid early-middle Miocene exhumation of the
603 Kazdağ Massif (western Anatolia). International Journal of Earth Science 98, 1935–1947.
604 doi:10.1007/s00531-008-0353-9

605 Christofides, G., Pécskay, Z., Eleftheriadis, G., Soldatos, T., Koroneos, A., 2004. The Tertiary
606 Evros volcanic rocks (Thrace, Northeastern Greece): Petrology and K/Ar Geochronology.
607 Geologica Carpathica 55, 397–409.

608 Delaloye, M., Bingöl, E., 2000. Granitoids from Western and Northwestern Anatolia:
609 Geochemistry and Modeling of Geodynamic Evolution, International Geology Review, 42,
610 241–268.

611 Dinter, D.A., 1998. Late Cenozoic extension of the Alpine collisional orogen, northeastern
612 Greece: Origin of the north Aegean basin. Geological Society of America Bulletin 110, 1208–
613 1230.

614 Dönmez, M., Akçay, A.E., Genç, Ş.C., Acar, Ş., 2005. Biga Yarımadasında Orta-Üst Eosen
615 Volkanizması ve Denizel İgnimbiritler. Bulletin of the Mineral Research and Exploration,
616 (Turkey) 131, 49–61. (*In Turkish)*

617 Duru, M., Pehlivan, Ş., Şentürk, Y., Yavaş, F., Kar, H., 2004. New Results on the
618 Lithostratigraphy of the Kazdağ Massif in Northwest Turkey. Turkish Journal of Earth
619 Sciences 13, 177–186.

620 Elmas, A., 2012. The Thrace Basin: stratigraphic and tectonic palaeogeographic evolution of
621 the Palaeogene formations of northwest Turkey. International Geology Review 54, 1419–
622 1442. doi: 10.1080/00206814.2011.644732

623 Elmas, A., Koralay, E., Duru, O., Schmidt, A., 2016. Geochronology, geochemistry, and
624 tectonic setting of the Oligocene magmatic rocks (Marmaros Magmatic Assemblage) in
625 Gökçeada Island, northwest Turkey. International Geology Review 59, 420-447.
626 doi.10.1080/00206814.2016.1227941

627 Ercan, T., Satir, M., Steinitz, G., Dora, A., Sarifakioglu, E., Adis, C., Walter, H.-J., Yildirim,
628 T., 1995. Biga yarımadası ile Gökçeada, Bozcaada ve Tavşan adalarındaki (KB Anadolu)
629 Tersiyer volkanizmasının özellikleri. Bulletin of the Mineral Research and Exploration,
630 (Turkey) 117, 55–86. (*In Turkish)*

631 Ercan, T., Türkecan, A., Guillou, H., Satır, M., Sevin, D., Şaroğlu, F., 1998. Marmara Denizi
632 çevresindeki Tersiyer volkanizmasının özellikleri. Bulletin of the Mineral Research and
633 Exploration, (Turkey) 120, 199–221. (*In Turkish)*

634 Erdoğan, B., Akay, E., Hasözbek, A., Satır, M., Siebel, W., 2013. Stratigraphy and tectonic
635 evolution of the Kazdağı Massif (NW Anatolia) based on field studies and radiometric ages.
636 International Geology Review 55, 2060–2082. doi: 10.1080/00206814.2013.818756

637 Erkül, F., Helvacı, C., Sözbilir, H., 2005. Stratigraphy and Geochronology of the Early
638 Miocene Volcanic Units in the Bigadiç Borate Basin, Western Turkey. Turkish Journal of
639 Earth Sciences 14, 227–253.

640 Ersoy, E.Y., Palmer, M.R. 2013. Eocene-Quaternary magmatic activity in the Aegean:
641 Implications for mantle metasomatism and magma genesis in an evolving orogeny. Lithos
642 180–181, 5–24. doi: 10.1016/j.lithos.2013.06.007

643 Ersoy, E.Y., Palmer, M.R., Uysal, İ., Gündoğan, İ., 2014. Geochemistry and petrology of the
644 Early Miocene lamproites and related volcanic rocks in the Thrace Basin, NW Anatolia.
645 Journal of Volcanology and Geothermal Research 283, 143–158.
646 doi:10.1016/j.jvolgeores.2014.06.016

647 Fornash, K.F., Cosca, M.A., Whitney, D.L., 2016. Tracking the timing of subduction and
648 exhumation using 40Ar/39Ar phengite ages in blueschist- and eclogite-facies rocks
649 (Sivrihisar, Turkey). Contributions to Mineralogy and Petrology 171, 67. doi:10.1007/s00410-
650 016-1268-2

651 Fytikas, M., Innocenti, F., Manetti, P., Mazzuoli, R., Peccerillo, A., Villari, L., 1984. Tertiary
652 to Quaternary evolution of volcanism in the Aegean region. Geological Society of London
653 Special Publication 17, 687–699.

654 Gallhofer, D., von Quadt, A., Peytcheva, I., Schmid, S.M., Heinrich, C.A., 2015. Tectonic,
655 magmatic, and metallogenic evolution of the Late Cretaceous arc in the Carpathian-Balkan
656 orogen. Tectonics 34, 1813–1836.

657 Genç, Ş.C., 1998. Evolution of the Bayramic¸ Magmatic Complex, Northwestern Anatolia.
658 Journal of Volcanology and Geothermal Research, 85, 233–249.

659 Genç, Ş.C., Dönmez, M., Akçay, A.E., Altunkaynak, Ş., Eyüpoğlu, M., Ilgar, Y., 2012. Biga
660 Yarımadası Tersiyer volkanizmasının stratigrafik, petrografik ve kimyasal özellikleri, in
661 Yüzer, E., Tunay, G., (Eds.), Biga Yarımadasının Genel ve Ekonomik Jeolojisi. Bulletin of
662 the Mineral Research and Exploration, Special Publications, 28, 122–162.

663 Genç, Ş.C., Yılmaz, Y., 1997. An example of postcollisional magmatism in Northwestern
664 Anatolia: the Kızderbent volcanic (Armutlu peninsula, Turkey). Turkish Journal of Earth
665 Science 6, 33–42.

666 Georgiev, S., Marchev, P., Heinrich, C.A., von Quadt, A., Peytcheva, I., Manetti, P., 2009.
667 Origin of Nepheline-normative High-K Ankaramites and the Evolution of Eastern
668 Srednogorie Arc in SE Europe. Journal of Petrology 50, 1899–1933.
669 doi:10.1093/petrology/egp056

670 Georgiev, S., von Quadt, A., Heinrich, C.A., Peytcheva, I., Marchev, P., 2012. Time evolution
671 of a rifted continental arc: Integrated ID-TIMS and LA-ICPMS study of magmatic zircons
672 from the Eastern Srednogorie, Bulgaria. Lithos 154, 53–67. doi:10.1016/j.lithos.2012.06.020

673 Gülmez, F., Genç, Ş.C., Keskin, M., Tüysüz, O., 2013. A post-collision slab-breakoff model
674 for the origin of the Middle Eocene magmatic rocks of the Armutlu–Almacık belt, NW
675 Turkey and its regional implications. Geological Society of London, Special Publications 372,
676 107–139. doi: 10.1144/SP372.12

677 Gülmez, F., Genç, Ş.C., Prelevic, D., Tüysüz, O., Karacık, Z., Roden, M.F., Billor, Z., 2016.
678 Ultrapotassic Volcanism from the Waning Stage of the Neotethyan Subduction: a Key Study

679 from the Izmir–Ankara–Erzincan Suture Belt, Central Northern Turkey. Journal of Petrology
680 57, 561–593. doi: 10.1093/petrology/egw021

681 Ilgar, A., Demirci-Sezen, E., Demirci, Ö., 2012. Biga Yarımadası Tersiyer İstifinin
682 Stratigrafisi ve sedimantolojisi, in Yüzer, E., Tunay, G., (Eds.), Biga Yarımadasının Genel ve
683 Ekonomik Jeolojisi. Bulletin of the Mineral Research and Exploration, Special Publications,
684 28, 122–162.

685 Jackson, S.E., Pearson, N.J., Griffin,W.L., Belousova, E.A., 2004. The application of laser
686 ablation-inductively coupled plasma mass spectrometry to in situ U/Pb zircon geochronology.
687 Chemical Geology 211, 47–69.

688 Jahn-Awe, S. Pleguer, J., Frei, D., Georgiev, N., Froitzheim, N., Nagel, T.J., 2012. Time
689 constraints for low-angle shear zones in the Central Rhodopes (Bulgaria) and their
690 significance for the exhumation of high-pressure rocks. International Journal of Earth Science
691 101, 1971–2004. doi:10.1007/s00531-012-0764-5

692 Jolivet, L., Brun, J.-P., 2010. Cenozoic geodynamic evolution of the Aegean. International
693 Journal of Earth Science 99, 109–138. doi:10.1007/s00531-008-0366-4

694 Kamenov, B., Tarassova, E., Nedialkov, R., Amov, B., Monchev, P., Mavroudchiev, B.,
695 2000. New radiometric data from Late Cretaceous plutons in the Eastern Srednogorie area,
696 Bulgaria. Geochemistry, Mineralogy and Petrology 37, 13–24.

697 Karacık, Z., Yılmaz, Y., Pearce, J.A., Ece, Ö.I., 2008. Petrochemistry of the south Marmara
698 granitoids, northwest Anatolia, Turkey. International Journal of Earth Sciences 97, 1181–
699 1200. doi:10.1007/s00531-007-0222-y

700 Kasapoğlu, B., Ersoy, E.Y., Uysal, İ., Palmer, M.R., Zack, T., Koralay, O.E., Karlsson, A.,
701 2016. The Petrology of Paleogene Volcanism in the Central Sakarya, Nallıhan Region (NW
702 Anatolia): Implications for the Initiation and Evolution of Post-Collisional, Slab Break-off
703 Related Magmatic Activity. Lithos 246–247, 81–98. doi:10.1016/j.lithos.2015.12.024

704 Kilias, A., Falalakis, G., Mountrakis, D., 1999. Cretaceous–Tertiary structures and kinematics
705 of the Serbomacedonian metamorphic rocks and their relation to the exhumation of the
706 Hellenic hinterland (Macedonia, Greece). International Journal of Earth Sciences 88, 513–
707 531.

Kilias, A., Falalakis, G., Sfeikos, A., Papadimitriou, E., Vamvaka, A., Gkarlaouni, C., 2013. The Thrace basin in the Rhodope province of NE Greece — A tertiary supradetachment basin and its geodynamic implications. Tectonophysics 595–596, 90–105. doi:10.1016/j.tecto.2012.05.008

Krushensky, R.D., 1976. Neogene calc-alkaline extrusive and intrusive rocks of the Karalar-Yesiller area. Bulletin Volcanologique 39, 336-360.

Kürkçüoğlu, B., Furman, T., Hanan, B., 2008. Geochemistry of postcollisional mafic lavas from the North Anatolian Fault zone, Northwestern Turkey. Lithos, 101, 416–434. doi:10.1016/j.lithos.2007.08.017

Liati A., Gebauer, D., Wysoczanski, R., 2002. U–Pb SHRIMP-dating of zircon domains from UHP garnet-rich mafic rocks and late pegmatoids in the Rhodope zone (N Greece); evidence for Early Cretaceous crystallization and Late Cretaceous metamorphism, Chemical Geology 184, 281–299.

Lips, A.L.W., White, S.H., Wijbrans, J.R., 2000. Middle-Late Alpine thermotectonic evolution of the southern Rhodope Massif, Greece, Geodinamica Acta, 13, 281–292.

Ludwig, K.R., 2003. User's Manual for Isoplot 3.0. Berkeley Geochronology Center. Special Publication 4.

Marchev, P., Georgiev, S., Raicheva, R., Peytcheva, I., von Quadt, A., Ovtcharova, M., Bonev, N., 2013. Adakitic magmatism in post-collisional setting: An example from the Early–Middle Eocene Magmatic Belt in Southern Bulgaria and Northern Greece. Lithos 180–181, 159–180. doi: 10.1016/j.lithos.2013.08.024

Marchev, P., Kibarov, P., Spikings, R., Ovtcharova, M., Márton, I., Moritz, R., 2010. $^{40}Ar/^{39}Ar$ and U-Pb geochronology of the Iran Tepe volcanic complex, Eastern Rhodopes. Geologica Balcanica 39, 3–12.

Marchev, P., Raicheva, R., Downes, H., Vaselli, O., Chiaradia, M., Moritz, R., 2004. Compositional diversity of Eocene–Oligocene basaltic magmatism in the Eastern Rhodopes, SE Bulgaria: implications for genesis and tectonic setting. Tectonophysics 393, 301– 328. doi:10.1016/j.tecto.2004.07.045

736 Marchev, P., Georgiev, S., Zajacz, Z., Manetti, P., Raicheva, R., von Quadt, A., Tommasini,
737 S., 2009. High-K ankaramitic melt inclusions and lavas in the Upper Cretaceous Eastern
738 Srednogorie continental arc, Bulgaria: Implications for the genesis of arc shoshonites. Lithos
739 113, 228–245. doi:10.1016/j.lithos.2009.03.014

740 Mposkos, E., Kostopoulos, D., 2001. Diamond, former coesite and supersilicic garnet in
741 metasedimentary rocks from the Greek Rhodope: a new ultrahigh-pressure metamorphic
742 province established. Earth and Planetary Science Letters 192, 497-506.

743 Naydenov, K., Peytcheva, I., von Quadt, A., Sarov, S., Kolcheva, K., Dimov, D., 2013. The
744 Maritsa strike-slip shear zone between Kostenets and Krichim towns, South Bulgaria —
745 Structural, petrographic and isotope geochronology study. Tectonophysics 595–596, 69–89.
746 doi: 10.1016/j.tecto.2012.08.005

747 Okay, A.I., Göncüoğlu, M.C., 2004. Karakaya Complex: a review of data and concepts.
748 Turkish Journal of Earth Science 13, 77–95.

749 Okay, A.I., Siyako, M. Bürkan, K.A. 1991. Geology and tectonic evolution of the Biga
750 peninsula, northwest Turkey. Bulletin of the Istanbul Technical University 44, 191-256.

751 Okay, A.I., Tansel, İ., Tüysüz, O., 2001. Obduction, subduction and collision as reflected in
752 the Upper Cretaceous–Lower Eocene sedimentary record of western Turkey. Geological
753 Magazine 138, 117–142.

754 Okay, A.I.,, İşintek, İ., Altıner, D., Özkan-Altıner, S., Okay, N., 2012. An olistostrome–
755 mélange belt formed along a suture: Bornova Flysch zone, western Turkey. Tectonophysics
756 568–569, 282–295. doi:10.1016/j.tecto.2012.01.007

757 Okay, A.I.,, Satır, M. 2000a. Upper Cretaceous Eclogite-Facies Metamorphic Rocks from the
758 Biga Peninsula, Northwest Turkey. Turkish Journal of Earth Sciences 9, 47–56.

759 Okay, A.I.,, Satır, M. 2000b. Coeval plutonism and metamorphism in a latest Oligocene
760 metamorphic core complex in northwest Turkey. Geological Magazine 138, 495–516.

761 Okay, A.I.,, Satır, M., Zattin, M., Cavazza, W., Topuz, G., 2008. An Oligocene ductile strike-
762 slip shear zone: The Uludağ Massif, northwest Turkey—Implications for the westward
763 translation of Anatolia. GSA Bulletin 120, 893–911. doi: 10.1130/B26229.1

764 Önen, A.P., 2003. Neotethyan ophiolitic rocks of the Anatolides of NW Turkey and
765 comparison with Tauride ophiolites. Journal of the Geological Society, London 160, 947–962.

766 Özcan, Z., Okay, A.I.,, Özcan, E., Hakyemez, A., Özkan-Altıner, S., 2012. Late Cretaceous–
767 Eocene Geological Evolution of the Pontides Based on New Stratigraphic and Palaeontologic
768 Data between the Black Sea Coast and Bursa (NW Turkey). Turkish Journal of Earth
769 Sciences 21, 933–960.

770 Peytcheva, I., von Quadt, A., Georgiev, N., Ivanov, Zh., Heinrich, C.A., Frank, M., 2008.
771 Combining trace-element compositions, U Pb geochronology and Hf isotopes in zircons to
772 unravel complex calcalkaline magma chambers in the Upper Cretaceous Srednogorie zone
773 (Bulgaria). Lithos 104, 405–427. doi:10.1016/j.lithos.2008.01.004

774 Peytcheva, I., von Quadt, A., Ovtcharova, M., Handler, R., Neubauer, F., Salnikova, E.,
775 Kostitsyn, Y., Sarov, S., Kolcheva, K., 2004. Metagranitoids from the eastern part of the
776 Central Rhodopean Dome (Bulgaria): U–Pb, Rb–Sr and $^{40}Ar/^{39}Ar$ timing of emplacement and
777 exhumation and isotope-geochemical features. Mineralogy and Petrology 82, 1–31.
778 doi:10.1007/s00710-004-0039-3

779 Pourteau, A., Oberhänsli, R., Candan, O., Barrier, E., Vrielynck, B., 2016. Neotethyan closure
780 history of western Anatolia: a geodynamic discussion. International Journal of Earth Sciences
781 105, 203–224. doi:10.1007/s00531-015-1226-7

782 Pourteau, A., Sudo, M., Candan, O., Lanari, P., Vidal, O., Oberhänsli, R., 2013. Neotethys
783 closure history of Anatolia: insights from 40Ar–39Ar geochronology and P–T estimation in
784 high-pressure metasedimentary rocks. Journal of Metamorphic Geology 31, 585–606. doi:
785 10.1111/jmg.12034

786 Ricou, L.E., Burg J.-P., Godfriaux, I., Ivanov, Z. 1998. Rhodope and vardar: the metamorphic
787 and the olistostromic paired belts related to the Cretaceous subduction under Europe.
788 Geodinamica Acta 11, 285–309.

789 Rieser, A.B., Neubauer, F., Handler, R., Velichkova, S.H., Ivanov, I., 2008. New 40Ar/39Ar
790 age constraints on the timing of magmatic events in the Panagyurishte region, Bulgaria. Swiss
791 Journal of Geosciences 101, 107–123. doi: 10.1007/s00015-007-1243-z

792 Ring, U., Layer, P.W., 2003. High-pressure metamorphism in the Aegean, eastern
793 Mediterranean: Underplating and exhumation from the Late Cretaceous until the Miocene to
794 Recent above the retreating Hellenic subduction zone. Tectonics 22, 1022.

795 Robertson, A.H.F., Ustaömer, T., 2004. Tectonic evolution of the Intra-Pontide suture zone in
796 the Armutlu Peninsula, NW Turkey. Tectonophysics 381, 175–209.

797 Schmidt A., Pourteau, A., Candan, O., Oberhansli, R., 2015. Lu–Hf geochronology on cm-
798 sized garnets using microsampling: New constraints on garnet growth rates and duration of
799 metamorphism during continental collision (Menderes Massif, Turkey). Earth and Planetary
800 Science Letters 432, 24–35. doi: 10.1016/j.epsl.2015.09.015

801 Şengör, A.M.C., Yılmaz, Y., 1981. Tethyan evolution of Turkey: a plate tectonic approach.
802 Tectonophysics 75, 181–241.

803 Singer, B., Marchev, P., 2000. Temporal evolution of arc magmatism and hydrothermal
804 activity, including epithermal gold veins, Borovitsa Caldera, Southern Bulgaria. Economic
805 Geology 95, 1155–1164.

806 Siyako, M., Huvaz, O., 2007. Eocene stratigraphic evolution of the Thrace Basin, Turkey.
807 Sedimentary Geology 198, 75–91. doi:10.1016/j.sedgeo.2006.11.008

808 Sláma, J., et al., 2008. Plešovice zircon — a new natural reference material for U–Pb and Hf
809 isotopic microanalysis. Chemical Geology 249, 1–35. doi: 10.1016/j.chemgeo.2007.11.005

810 Sunal, G., Satır, M., Natal'in, B.A., Topuz, G., Vonderschmidt, O., 2011. Metamorphism and
811 diachronous cooling in a contractional orogen: the Strandja Massif, NW Turkey. Geological
812 Magazine 148, 580–596. doi:10.1017/S0016756810001020

813 Türkoğlu, E., Zulauf, G., Linckens, J., Ustaömer, T., 2016. Dextral strike‐slip along the
814 Kapıdağ shear zone (NW Turkey): evidence for Eocene westward translation of the Anatolian
815 plate. International Journal of Earth Science. 105, 2061–2073. doi: 10.1007/s00531-016-
816 1372-6

817 Ustaömer, P.A., Ustaömer, T., Collins, A.S., Reischpeitsch, J, 2009. Lutetian arc-type
818 magmatism along the southern Eurasian margin: New U-Pb LA-ICPMS and whole-rock

819 geochemical data from Marmara Island, NW Turkey. Mineralogy and Petrology 96, 177–196.
820 doi: 10.1007/s00710-009-0051-8

821 van Hinsbergen, D.J.J., Hafkenscheid, E., Spakman, W., Meulenkamp, J.E., Wortel, R., 2005.
822 Nappe stacking resulting from subduction of oceanic and continental lithosphere below
823 Greece. Geology 33, 325–328. doi: 10.1130/G20878.1

824 von Quadt, A., Moritz, R., Peytcheva, I., Heinrich, C., 2005. Geochronology and
825 geodynamics of Late Cretaceous magmatism and Cu–Au mineralization in the Panagyurishte
826 region of the Apuseni–Banat–Timok–Srednogorie belt (Bulgaria). Ore Geology Reviews 27,
827 95–126. doi:10.1016/j.oregeorev.2005.07.024

828 Wawrzenitz N., Krohe, A., 1998. Exhumation and doming of the Thasos metamorphic core
829 complex (S Rhodope, Greece): structural and geochronological constraints. Tectonophysics
830 285, 301–332.

831 Wawrzenitz N., Mposkos, E., 1997. First evicence for Lower Cretaceous HP/HT-
832 metamorphism in the eastern Rhodope, North Aegean region, North-east Greece. European
833 Journal of Mineralogy 9, 659–664.

834 Wiedenbeck, M., Alle, P., Corfu, F., Griffin, W.L., Meier, M., Oberli, F., von Quadt, A.,
835 Roddick, J. C., Spiegel, W., 1995. Three natural zircon standards for U-Th-Pb, Lu-Hf, trace
836 element and REE analyses. Geostandards Newsletter 19, 1–23.

837 Yaltırak, C., 2002. Tectonic evolution of the Marmara Sea and its surroundings. Marine
838 Geology 190, 493–529.

839 Yılmaz, Y., Genç, Ş.C., Karacık, Z., Altunkaynak, Ş., 2001, Two contrasting magmatic
840 associations of NW Anatolia and their tectonic significance, Journal of Geodynamics, 31,
841 243–271.

842 Yılmaz, Y., Polat, A., 1998. Geology and Evolution of the Thrace Volcanism, Turkey. Acta
843 Vulcanologica 10, 293–303.

844 Zachariadis, P., 2007. Ophiolites of the eastern Vardar Zone, N. Greece. PhD dissertation
845 Mainz: Johannes Gutenberg-Universität, 131 p.

846

Figure Captions

Figure 1. Simplified geological map of NW Anatolia – Northern Aegean region showing the main tectonic units and tectonic elements of the region. Dark green colors represent the ophiolitic rocks. The major extensional detachment faults are Mesta (*or* Ribonovo) (MDF), Strymon (StDF) and Kerdilion detachment faults (KDF) in the Rhodope extensional province and Gediz (GDF) and Simav (SiDF) detachment faults in the West Anatolia extensional province. The major extensional domes (or core complexes) are Central Rhodope (*or* Arda) Dome (CRD), Kesebir-Kardamos Dome (KKD), Byala-Reka Kechros Dome (BRKD) and Southern Rhodope Core Complex (SRCC) in the Rhodopes, and Menderes Massif and Kazdağ Core Complexes (KCC) in Western Anatolia. VS: Vardar suture, IPS: Intra-Pontide suture; IAS: İzmir-Ankara suture; MSZ: Maritza Shear Zone, USZ: Uludağ shear zone; EFZ: Eskişehir fault zone; NAFZ: North Anatolian Fault zone. Compiled from the studies referenced in the Geological Setting section in the text.

Figure 2. Simplified geological map of the NW Anatolia – Northern Aegean region showing the distribution of the Upper Cretaceous to Recent magmatic products and the major tectonic elements in the region. The numbers on the magmatic units represent the ranges of published radiometric age data. The red numbers refer to the Na-alkaline OIB-type basaltic products. Abbreviations are same as in the Figure 1 (additionally: İBTZ: İzmir-Balıkesir Transfer zone, FBFZ: Fethiye-Burdur fault zone).

Figure 3. Geological map of the Biga Peninsula and its environs in NW Anatolia. ADF and ŞDF refer to Alakaçi and Şelale detachment faults which controlled the Late Oligocene to Miocene exhumation of the Kazdağ metamorphic massif. U-Pb zircon ages of this study are shown in squares. ADF: Alakeçi detachment fault, ŞDF: Şelale detachment fault, KSZ: Kapıdağ shear zone. The plutons are EVP: Evciler, KBP: Krabiga, İDP: İlyasdağ, KDP:

Kapıdağ, KSP: Kestanbol, EYP: Eybek and ILP: Ilıca plutons. See Supplementary Material 1 for the age references.

Figure 4. Simplified geological map of the Armutlu-Almacık-Nallıhan region. The plutons are: Ar: Armutlu, Gy: Gürgenyayla, Or: Orhaneli, Te: Tepeldağ, Tk: Topkaya, To: Topuk, Ul: Uludağ granitoids. USZ: Uludağ shear zone. See Supplementary Material 1 for the age references.

Figure 5. Generalized columnar sections for the Late Mesozoic to Cenozoic stratigraphy of the Armutlu-Almacık and Nallıhan regions.

Figure 6. U-Pb isotopic compositions for zircons from the samples of the Balıklıçeşme volcanics. See Supplementary Material 2 for the data.

Figure 7. U-Pb isotopic compositions for zircons from the samples of the Kirazlı volcanics. See Supplementary Material 2 for the data.

Figure 8. U-Pb isotopic compositions for zircons from the samples of the Hallaçlar and Dedetepe volcanics. See Supplementary Material 2 for the data.

Figure 9. Generalized columnar section of the Cenozoic stratigraphy of the Biga peninsula. See Supplementary Material 1 for the age references.

Figure 10. Compilation of the radiometric age data from the metamorphic, plutonic and volcanic rocks from the Rhodope, Biga, Thrace and Armutlu-Almacık-Nallıhan regions. See text for details.

Figure 11. Late Cretaceous to Oligocene geodynamic model for the northern Aegean region. See text for detailed discussions.

Table 1

Click here to download Table: Ersoy et al Table 1.doc

Table 1. Summary of the petrographic features and zircon U-Pb ages of the analysed samples

Volcanic Units	Member	sample	Location (UTM/UPS-europe 1979)		Rock type	Mineralogy	Texture	Alteration	Zircon Morphology	U-Pb Ages (Ma)
BALIKLIÇEŞME	Yeniköy	**C-42**	35S	0466010 4432014	Andesite-dacite	Pl, Am, Qtz, Ap, Zr, Op	hypocyrstalline porphyritic with glassy matrix	weak chloritization of amphiboles rare sosuritization of plagioclases	euhedral - magmatic zoning – w/l:75-150/200-450 µm	43.15 ± 0.27
	Bilaller	**C-12**	35S	0477577 4411036	Cpx-andesite	Pl, Cpx, Ap, Zr, Op	hypocyrstalline hyaloplitic	-	euhedral - magmatic zoning w/l:100-150/200-400 µm	37.92 ± 0.24
	Hacıbekirler	**C-16**	35S	0480775 4415856	Dacite	Pl, Bi, Qtz, Ap, Zr, Op	hypocyrstalline porphyritic with glassy matrix	weak chloritization of biotite rare sosuritization of plagioclases	euhedral - magmatic zoning w/l:75-200/200-350 µm	37.66 ± 0.69
	Beyçayırı	**B-11**	35S	0500469 4459685	Dacite	Pl, Bi, Am, Qtz, Ap, Zr, Op	hypocyrstalline porphyritic with glassy matrix	fresh	euhedral - magmatic zoning w/l:60-150/150-320 µm	35.75 ± 0.23
	undefined	**C-35**	35S	0473863 4421645	Andesite	Pl, Bi, Am, Ap, Zr, Op	hypocyrstalline microlitic	highly altered biotites & amphiboles	euhedral - magmatic zoning w/l:100-150/150-300 µm	40.24 ± 0.34
		C-17	35S	0471597 4428150	Andesite	Pl, Bi, Am, Ap, Zr, Op, Ep	hypocyrstalline porphyritic with glassy matrix	highly altered plagioclases, biotites & amphiboles (sosuritization & chloritization)	euhedral - magmatic zoning w/l:80-150/200-400 µm	36.38 ± 0.23
		C-41	35S	0461616 4435697	Dacite-rhyolite	Pl, Am, Qtz, Ap, Zr, Op	hypocyrstalline porphyritic with glassy matrix	slightly silicified	euhedral - magmatic zoning w/l:70-150/100-320 µm	37.29 ± 0.77
		B-20	35S	0486294 4467253	Andesite	Pl, Cpx, Ap, Zr, Op	hypocyrstalline porphyritic with glassy matrix	--	euhedral - magmatic zoning w/l:70-150/100-200 µm	35.09 ±1.0
KİRAZLI		**C-3/B**	35S	0461616 4435697	Basalt	Pl, Cpx, Ap, Zr, Op	hypocyrstalline microlitic	Intense sosuritization of plagioclase phenocrsyts	euhedral - magmatic zoning w/l:70-100/200-400 µm	32.71 ± 0.65
	Saraycık	**C-10**	35S	0479910 4404004	Rhyolite	Pl, Sa, Bi, Qtz, Ap, Zr, Op	hypocrystalline vitrofiric, spherulitic glassy matrix	silicified	euhedral - magmatic zoning w/l:50-75/70-100 µm	32.04 ± 0.31
	Atikhisar	**C-1/B**	35S	0460023 4442046	Rhyolite	Pl, Sa, Bi, Ap, Zr, Op	hypocyrstalline hyalopilitic	fresh	euhedral - magmatic zoning w/l:60-150/150-600 µm	31.05 ± 0.22
	Kızıldam	**B-36**	35S	0486093 4456158	Cpx-Andesite	Pl, Bi, Cpx, Ap, Zr, Op	hypocyrstalline porphyritic	quite fresh and has slightly altered cpx phenocrysts	euhedral - magmatic zoning w/l:60-200/100-310 µm	30.54 ± 0.21
	Dededağ	**B-23**	35S	0485000 4450062	Rhyolite	Pl, Sa, Bi, Ap, Zr, Op	Glassy matrix	intensely altered; chloritization & sosuritization	euhedral - magmatic zoning w/l:50-200/150-600 µm	31.42 ± 0.22
	Dededağ	**B-21**	35S	0477628 4444050	Rhyolite	Pl, Sa, Qtz, Ap, Zr, Op	hypocyrstalline felsitic	silisified glassy matrix and partly sosuritized plagioclase phenocrysts	euhedral - magmatic zoning w/l:100-150/100-200 µm	29.74 ± 0.64
	Dededağ	**B-29**	35S	0479850 4448199	Andesite	Pl, Bi, Ap, Zr, Op	hypocyrstalline porphyritic	intensive sosuritization of plagioclase	euhedral - magmatic zoning w/l:70-150/100-300 µm	31.24 ± 0.23

	undefined	**C-46**	35S	0492425 4431187	Rhyolite	Pl, Sa, Qtz, Ap, Zr, Op	hypocyrstalline felsitic	silicified	euhedral - magmatic zoning w/l:75-150/100-300 μm	30.76 ± 0.21
		C-18	35S	0488913 4421387	Andesite	Pl, Am, Bi, Ap, Zr, Op, Ep	hypocyrstalline trachytic	quite fresh slightly chloritized clinopyroxene microchryts	euhedral - magmatic zoning w/l:50-100/100-200 μm	27.47 ± 0.18
		C-20	35S	0489399 4422682	Andesite	Pl, Bi, Am, Ap, Zr, Op	hypocyrstalline porphyritic with glassy matrix	quite fresh slightly chloritized clinopyroxene microchryts	euhedral - magmatic zoning w/l:70-100/150-300 μm	26.81 ± 0.14
HALLAÇLAR	undefined	**HG-1**	35S	0525684 4382673	Andesite-dacite	Pl, Bi, Ap, Zr, Op	hypocyrstalline with glassy matrix	moderate sosuritization in plagoclase and glass matrix	euhedral - magmatic zoning w/l:100-150/200-300 μm	24.09 ± 0.55
		HG-2	35S	0530735 4307610	Andesite-dacite	Pl, Bi, Cpx, Ap, Zr, Op	hypocyrstalline porphyritic with glassy matrix	fresh	euhedral - magmatic zoning w/l:100-210/200-320 μm	24.75 ± 0.17
		HG-9	35S	0536865 4436733	Andesite-dacite	Pl, Bi, Cpx, Ap, Zr, Op	hypocyrstalline trachytic	fresh	euhedral - magmatic zoning w/l:100-150/150-300 μm	23.59 ± 0.49
		HG-12	35S	0524041 4396570	Andesite-dacite	Pl, Bi, Am, Ap, Zr, Op	hypocyrstalline porphyritic	intensive sosuritization of plagioclase and oxidation of amphiboles	euhedral - magmatic zoning w/l:100-200/100-300 μm	24.74 ± 0.14
		HG-13	35S	0505751 4372830	Andesite-dacite	Pl, Bi, Qtz, Ap, Zr, Op	hypocyrstalline porphyritic with glassy matrix	chloritization in glass matrix	euhedral - magmatic zoning w/l:100-200/200-300 μm	24.74 ± 0.23
DEDETEPE	undefined	**HG-3**	35S	0529947 4419204	Andesite-dacite	Pl, Bi, Am, Ap, Zr, Op	hypocyrstalline porphyritic with glassy microlitic matrix	fresh	euhedral - magmatic zoning w/l:100-250/200-310 μm	22.47 ± 0.52

Figure 1

Click here to download high resolution image

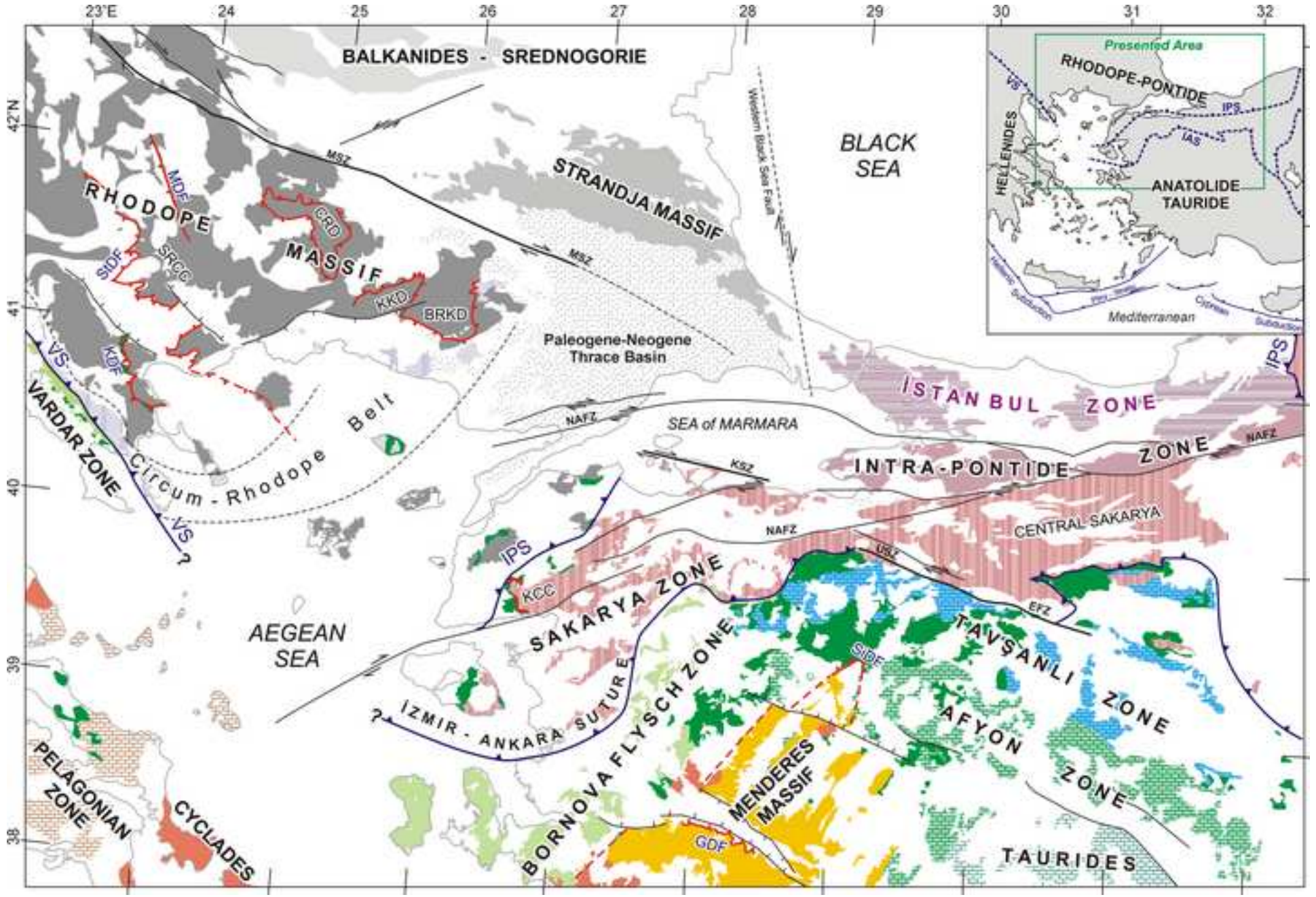

Figure 2

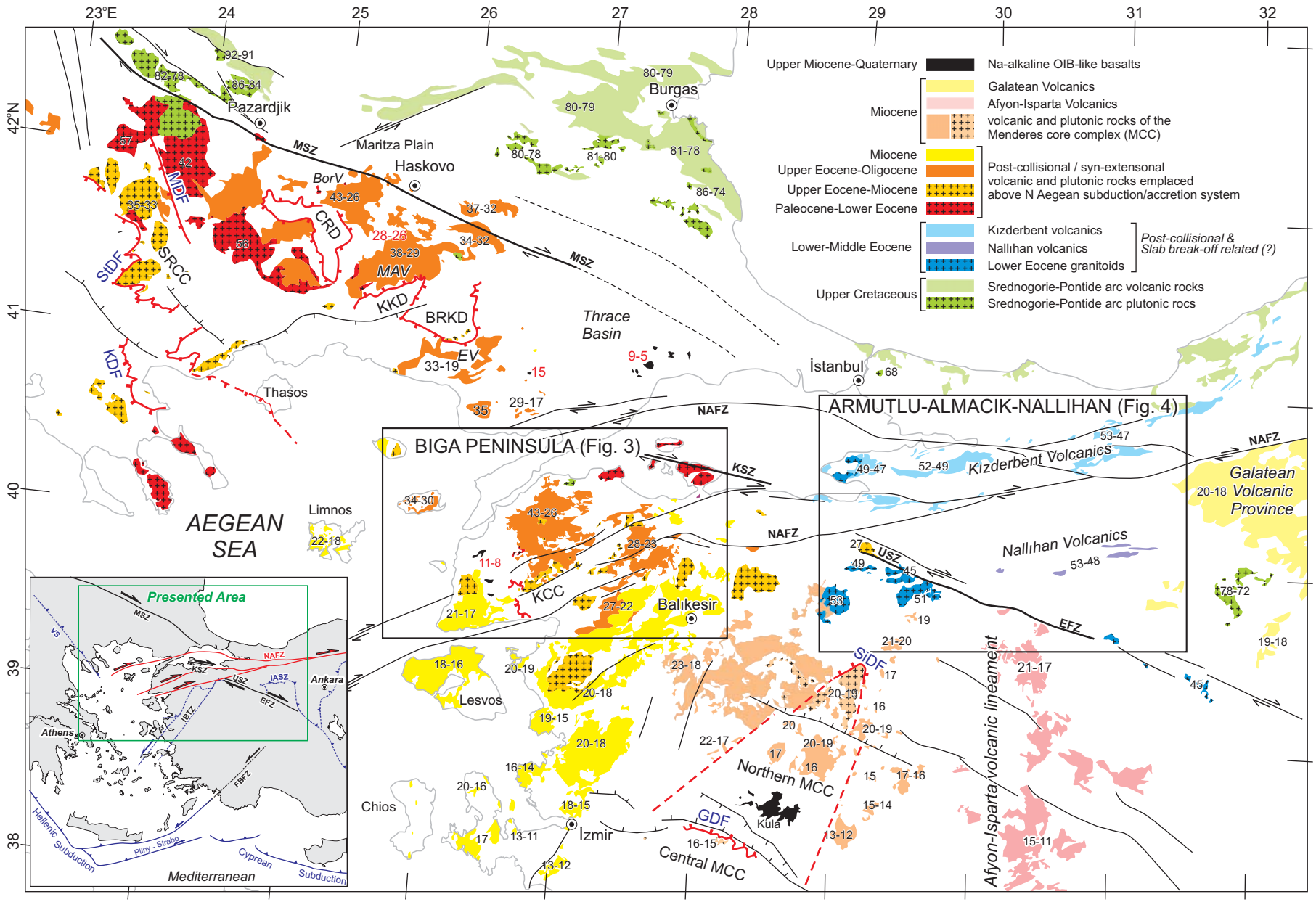
23°E
24
25
26
27
28
29
30
31
32
42°N
41
40
39
38
Upper Miocene-Quaternary
Na-alkaline OIB-like basalts
Miocene
Galatean Volcanics
Afyon-Isparta Volcanics
volcanic and plutonic rocks of the Menderes core complex (MCC)
Miocene
Upper Eocene-Oligocene
Upper Eocene-Miocene
Paleocene-Lower Eocene
Post-collisional / syn-extensional volcanic and plutonic rocks emplaced above N Aegean subduction/accretion system
Lower-Middle Eocene
Kızderbent volcanics
Nallıhan volcanics
Lower Eocene granitoids
Post-collisional & Slab break-off related (?)
Upper Cretaceous
Srednogorie-Pontide arc volcanic rocks
Srednogorie-Pontide arc plutonic rocs
Pazardjik
Maritza Plain
Haskovo
Burgas
Thrace Basin
İstanbul
Thasos
Limnos
AEGEAN SEA
Lesvos
Chios
Balıkesir
İzmir
Kula
Northern MCC
Central MCC
GDF
SiDF
MDF
SRCC
CRD
KKD
BRKD
EV
MAV
BorV
KDF
MSZ
NAFZ
KSZ
USZ
EFZ
KCC
Afyon-Isparta volcanic lineament
Galatean Volcanic Province
Kizderbent Volcanics
Nallıhan Volcanics
BIGA PENINSULA (Fig. 3)
ARMUTLU-ALMACIK-NALLIHAN (Fig. 4)
Presented Area
Ankara
Athens
Hellenic Subduction
Pliny - Strabo
Cyprean Subduction
Mediterranean

Figure 3

Click here to download high resolution image

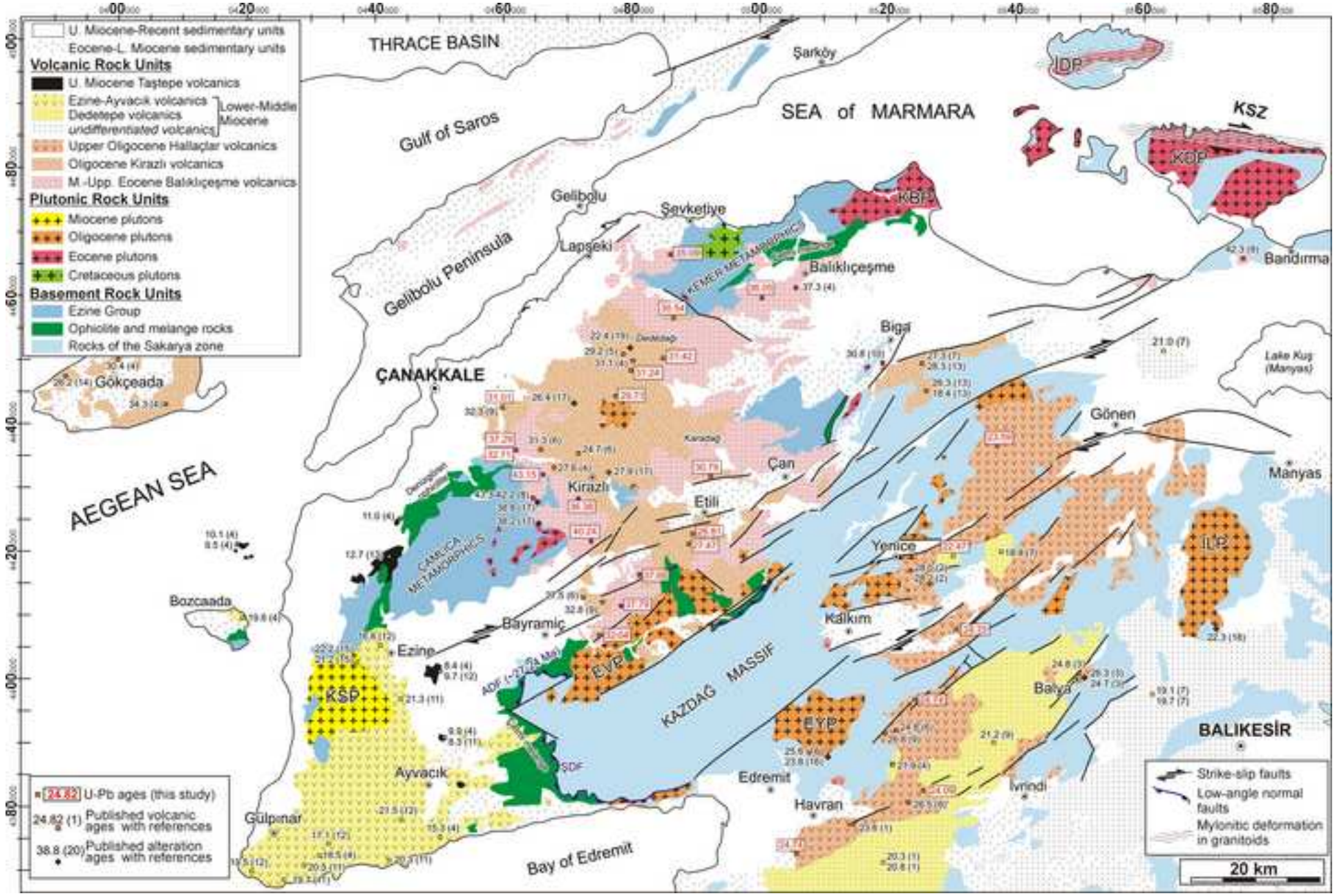

Figure 4

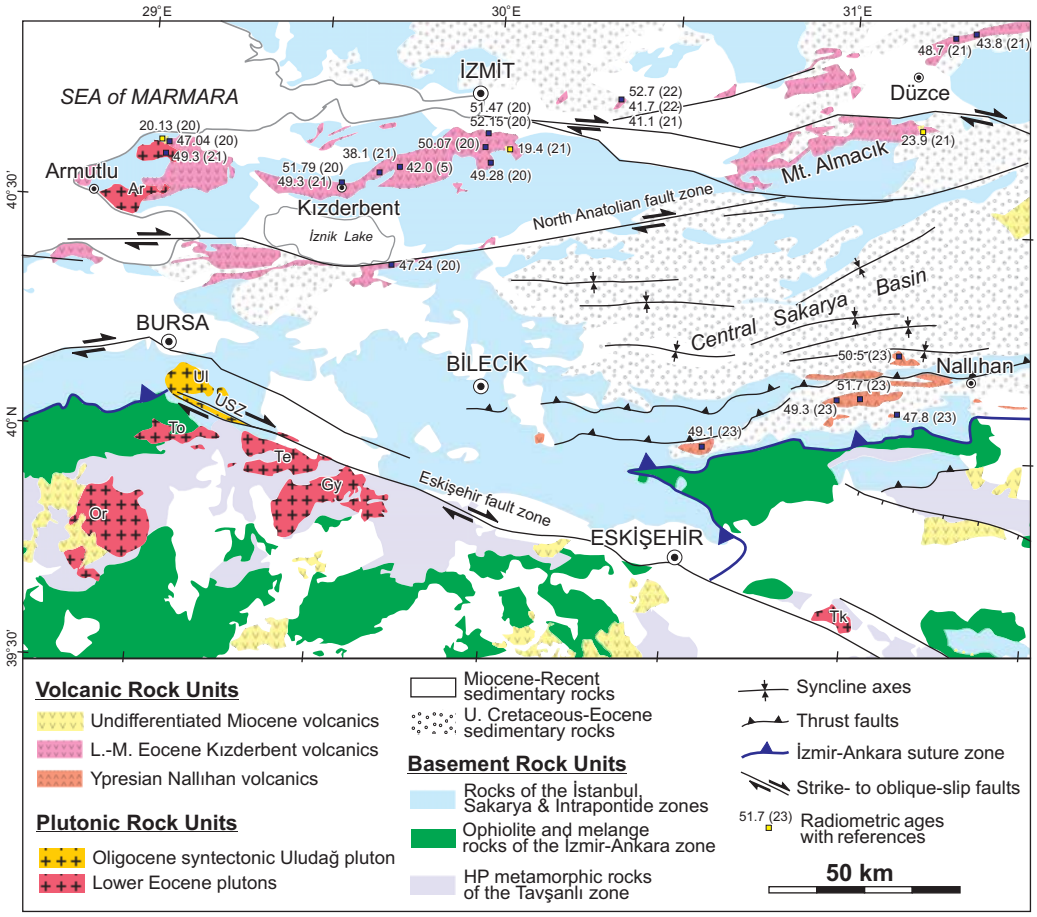
29° E
30° E
31° E
40° 30'
40° N
39° 30'
SEA of MARMARA
İZMİT
Düzce
Armutlu
Ar
Kızderbent
İznik Lake
BURSA
BİLECİK
ESKİŞEHİR
Nallıhan
Mt. Almacık
North Anatolian fault zone
Central Sakarya Basin
Eskişehir fault zone
USZ
Ul
To
Te
Cy
Or
Tk
20.13 (20)
47.04 (20)
49.3 (21)
51.79 (20)
49.3 (21)
38.1 (21)
42.0 (5)
50.07 (20)
52.15 (20)
51.47 (20)
19.4 (21)
49.28 (20)
52.7 (22)
41.7 (22)
41.1 (21)
48.7 (21)
43.8 (21)
23.9 (21)
47.24 (20)
50.5 (23)
51.7 (23)
49.3 (23)
47.8 (23)
49.1 (23)
Volcanic Rock Units
Undifferentiated Miocene volcanics
L.-M. Eocene Kızderbent volcanics
Ypresian Nallıhan volcanics
Plutonic Rock Units
Oligocene syntectonic Uludağ pluton
Lower Eocene plutons
Miocene-Recent sedimentary rocks
U. Cretaceous-Eocene sedimentary rocks
Basement Rock Units
Rocks of the İstanbul, Sakarya & Intrapontide zones
Ophiolite and melange rocks of the İzmir-Ankara zone
HP metamorphic rocks of the Tavşanlı zone
Syncline axes
Thrust faults
İzmir-Ankara suture zone
Strike- to oblique-slip faults
51.7 (23) Radiometric ages with references
50 km

Figure 5

Click here to download high resolution image

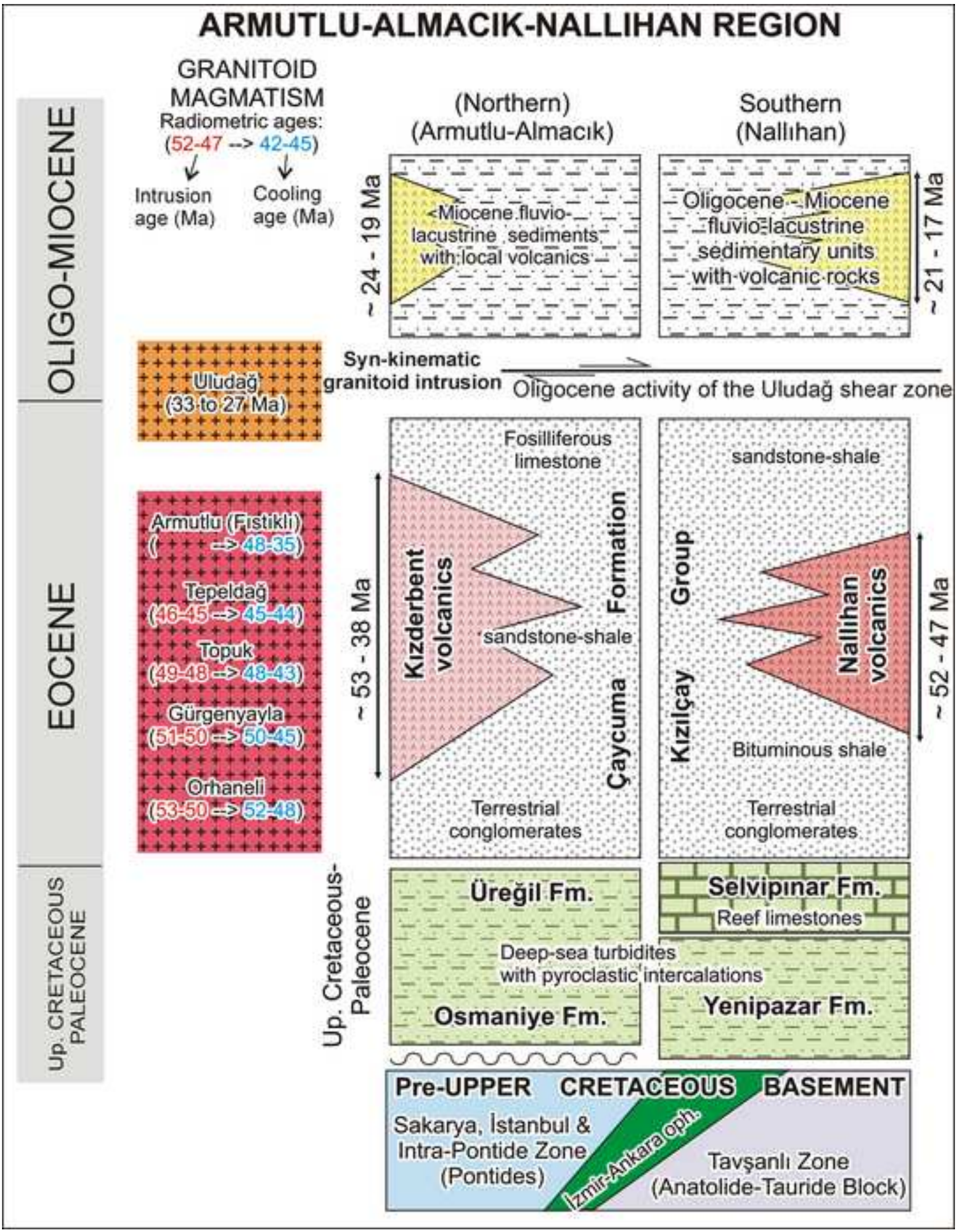

Figure 6

Click here to download high resolution image

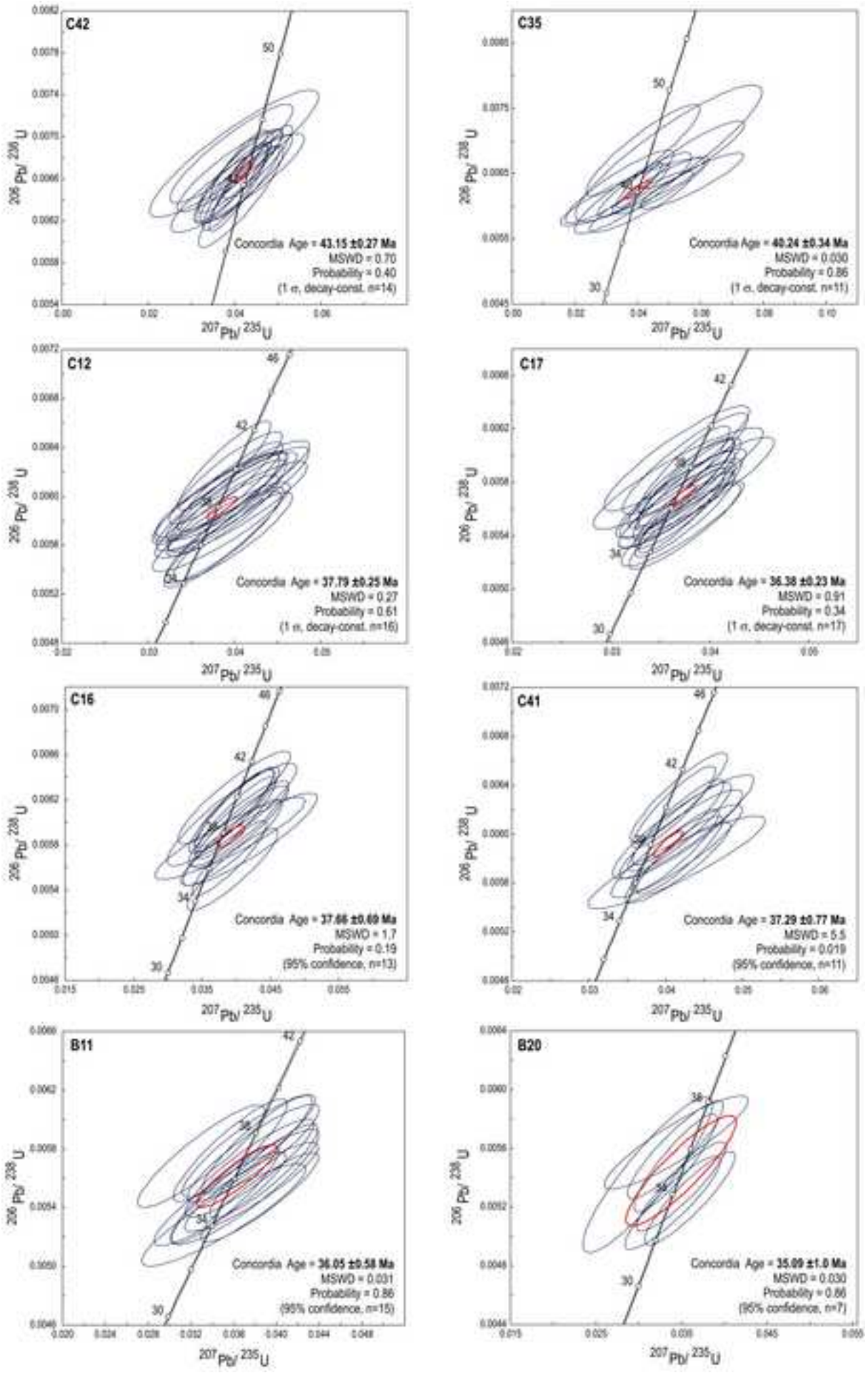

Figure 7

Click here to download high resolution image

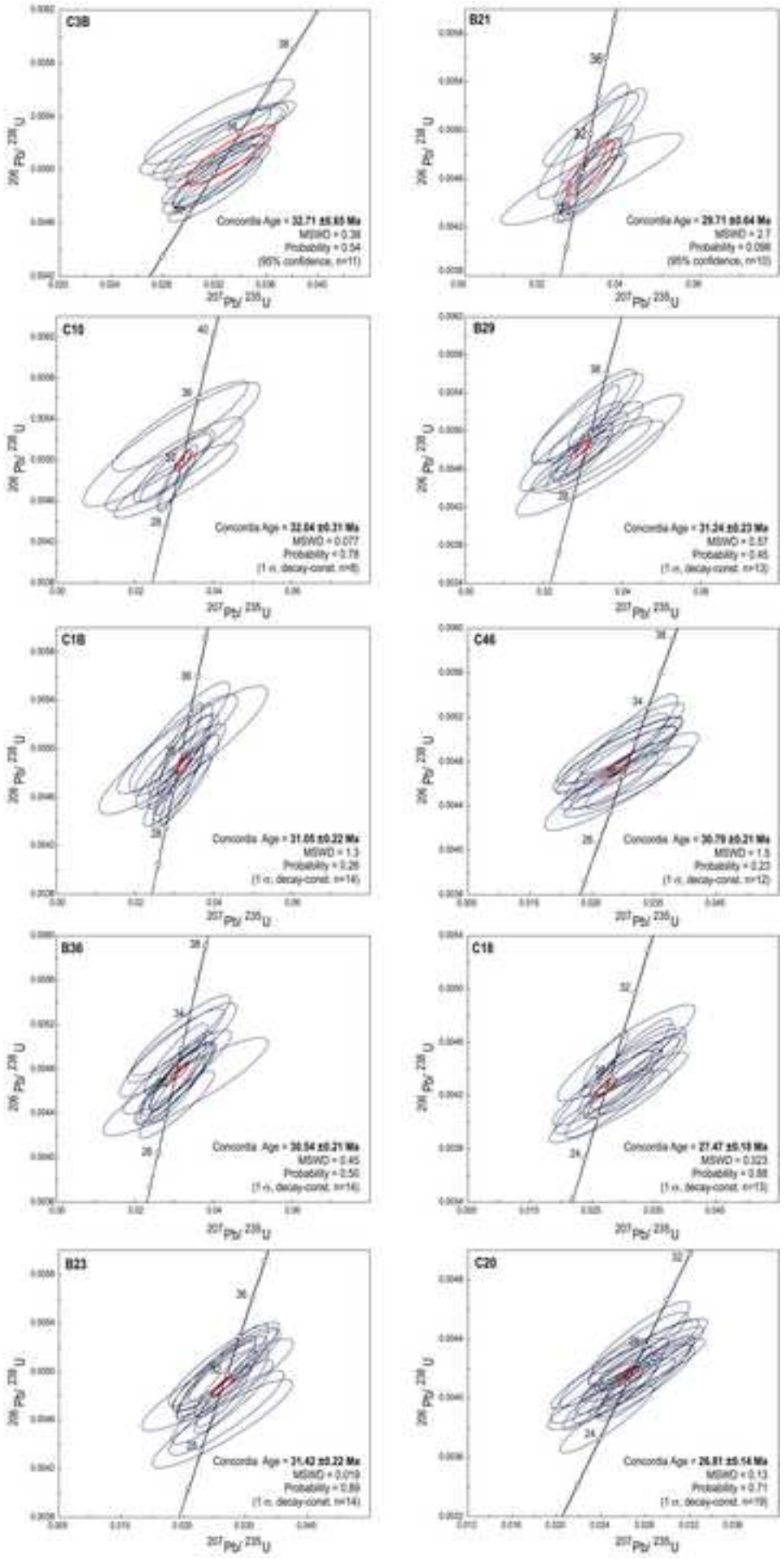

Figure 8

Click here to download high resolution image

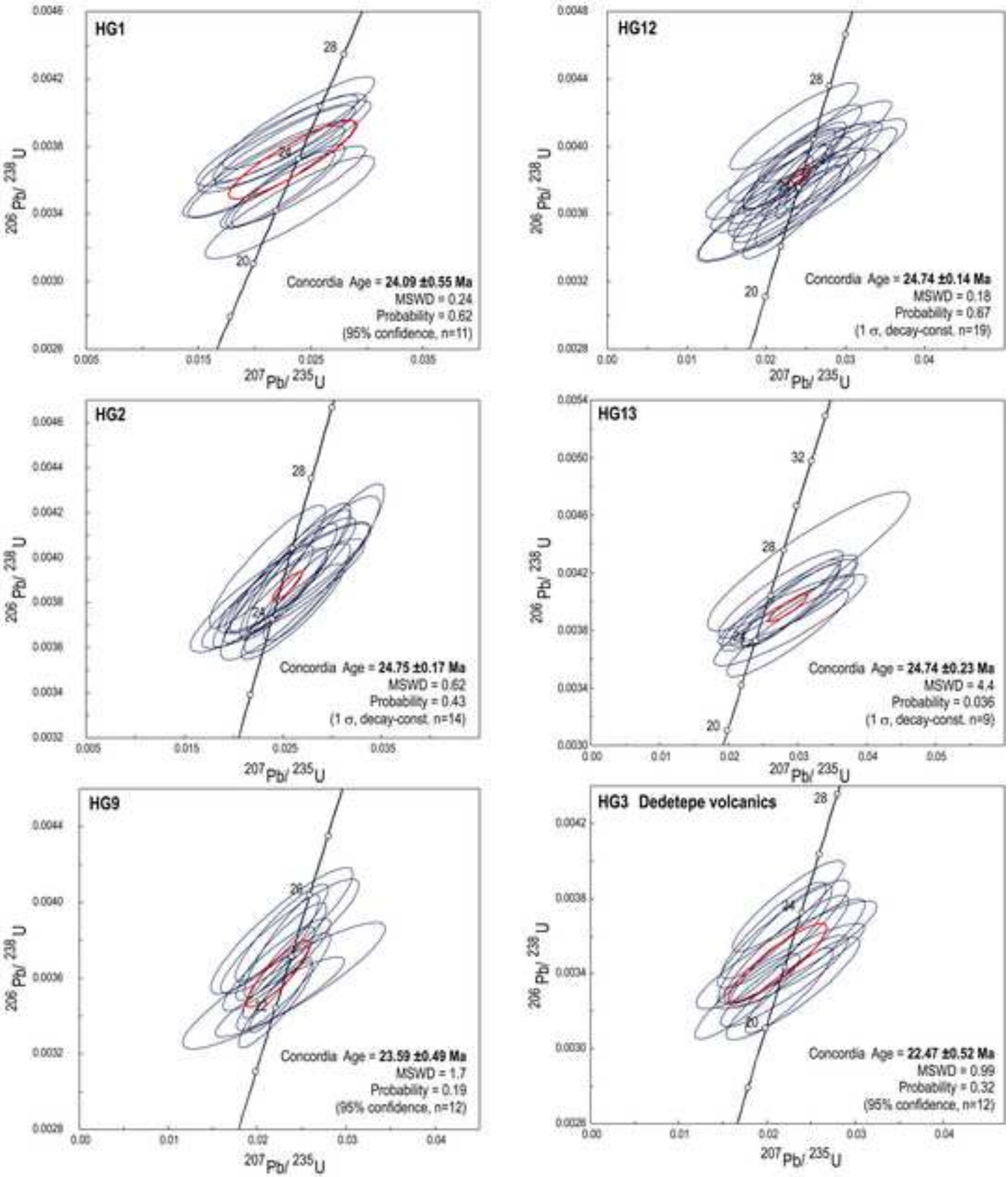

Figure 9

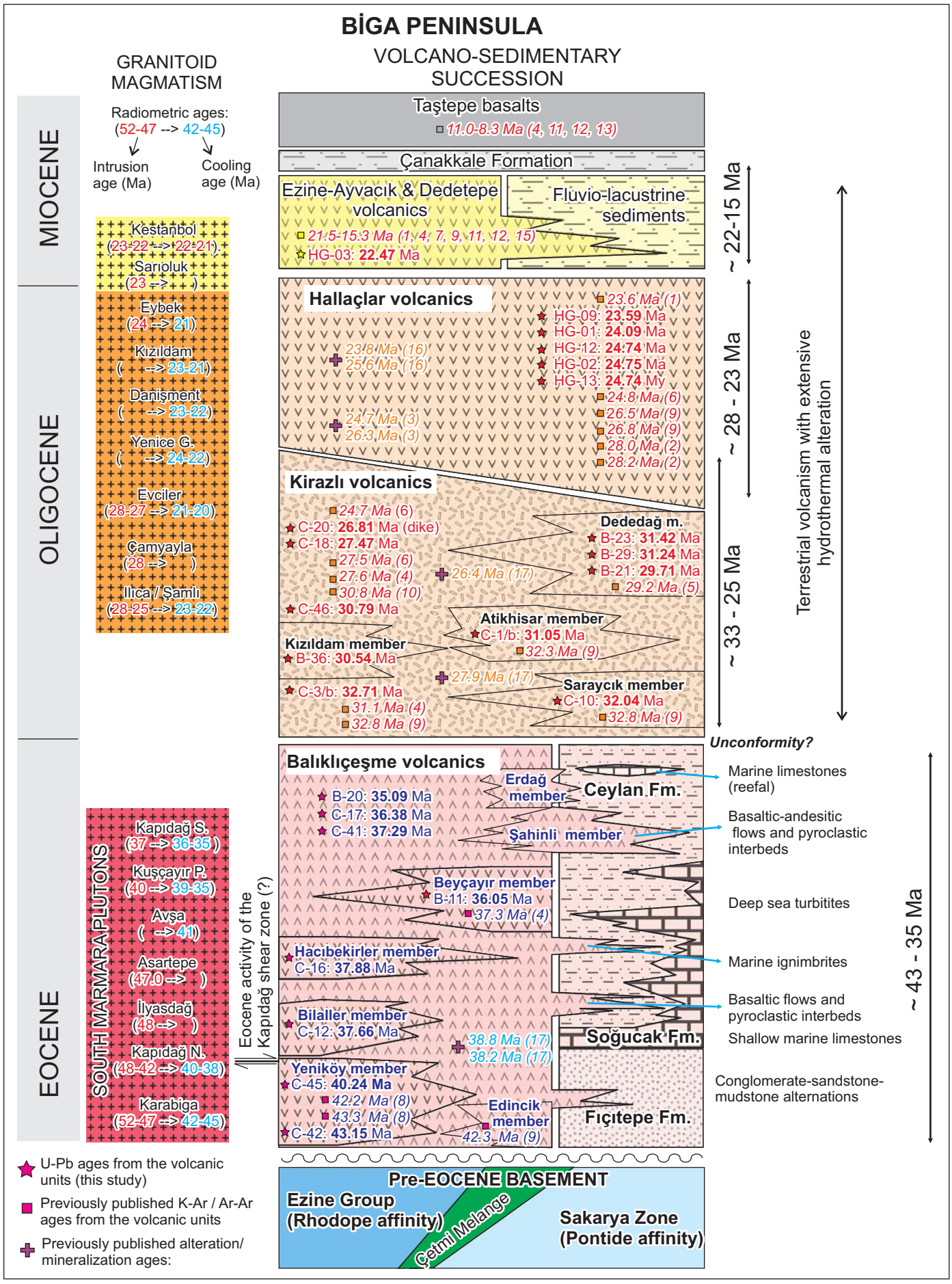
BİGA PENINSULA
GRANITOID MAGMATISM
VOLCANO-SEDIMENTARY SUCCESSION
MIOCENE
OLIGOCENE
EOCENE
Radiometric ages:
(52-47 --> 42-45)
Intrusion age (Ma)
Cooling age (Ma)
Kestanbol (23-22 --> 22-21)
Sarıoluk (23 -->)
Eybek (24 --> 21)
Kızıldam (--> 23-21)
Danişment (--> 23-22)
Yenice G. (--> 24-22)
Evciler (28-27 --> 21-20)
Çamyayla (28 -->)
Ilıca / Şamlı (28-25 --> 23-22)
SOUTH MARMARA PLUTONS
Kapıdağ S. (37 --> 36-35)
Kuşçayır P. (40 --> 39-35)
Avşa (--> 41)
Asartepe (47.0 -->)
İlyasdağ (48 -->)
Kapıdağ N. (48-42 --> 40-38)
Karabiga (52-47 --> 42-45)
Eocene activity of the Kapıdağ shear zone (?)
Taştepe basalts
11.0-8.3 Ma (4, 11, 12, 13)
Çanakkale Formation
Ezine-Ayvacık & Dedetepe volcanics
21.5-15.3 Ma (1, 4, 7, 9, 11, 12, 15)
HG-03: 22.47 Ma
Fluvio-lacustrine sediments
~ 22-15 Ma
Hallaçlar volcanics
23.6 Ma (1)
HG-09: 23.59 Ma
HG-01: 24.09 Ma
HG-12: 24.74 Ma
HG-02: 24.75 Ma
HG-13: 24.74 My
24.8 Ma (6)
26.5 Ma (9)
26.8 Ma (9)
28.0 Ma (2)
28.2 Ma (2)
23.8 Ma (16)
25.6 Ma (16)
24.7 Ma (3)
26.3 Ma (3)
~ 28 - 23 Ma
Kirazlı volcanics
24.7 Ma (6)
C-20: 26.81 Ma (dike)
C-18: 27.47 Ma
27.5 Ma (6)
27.6 Ma (4)
30.8 Ma (10)
C-46: 30.79 Ma
26.4 Ma (17)
Dededağ m.
B-23: 31.42 Ma
B-29: 31.24 Ma
B-21: 29.71 Ma
29.2 Ma (5)
Atikhisar member
C-1/b: 31.05 Ma
32.3 Ma (9)
Kızıldam member
B-36: 30.54 Ma
27.9 Ma (17)
C-3/b: 32.71 Ma
31.1 Ma (4)
32.8 Ma (9)
Saraycık member
C-10: 32.04 Ma
32.8 Ma (9)
~ 33 - 25 Ma
Terrestrial volcanism with extensive hydrothermal alteration
Unconformity?
Balıklıçeşme volcanics
Erdağ member
B-20: 35.09 Ma
C-17: 36.38 Ma
C-41: 37.29 Ma
Ceylan Fm.
Marine limestones (reefal)
Şahinli member
Basaltic-andesitic flows and pyroclastic interbeds
Beyçayır member
B-11: 36.05 Ma
37.3 Ma (4)
Deep sea turbitites
Hacıbekirler member
C-16: 37.88 Ma
Marine ignimbrites
Bilaller member
C-12: 37.66 Ma
Basaltic flows and pyroclastic interbeds
38.8 Ma (17)
38.2 Ma (17)
Soğucak Fm.
Shallow marine limestones
Yeniköy member
C-45: 40.24 Ma
42.2 Ma (8)
43.3 Ma (8)
C-42: 43.15 Ma
Edincik member
42.3 Ma (9)
Fıçıtepe Fm.
Conglomerate-sandstone-mudstone alternations
~ 43 - 35 Ma
Pre-EOCENE BASEMENT
Ezine Group (Rhodope affinity)
Çetmi Melange
Sakarya Zone (Pontide affinity)
U-Pb ages from the volcanic units (this study)
Previously published K-Ar / Ar-Ar ages from the volcanic units
Previously published alteration/ mineralization ages:

Figure 10

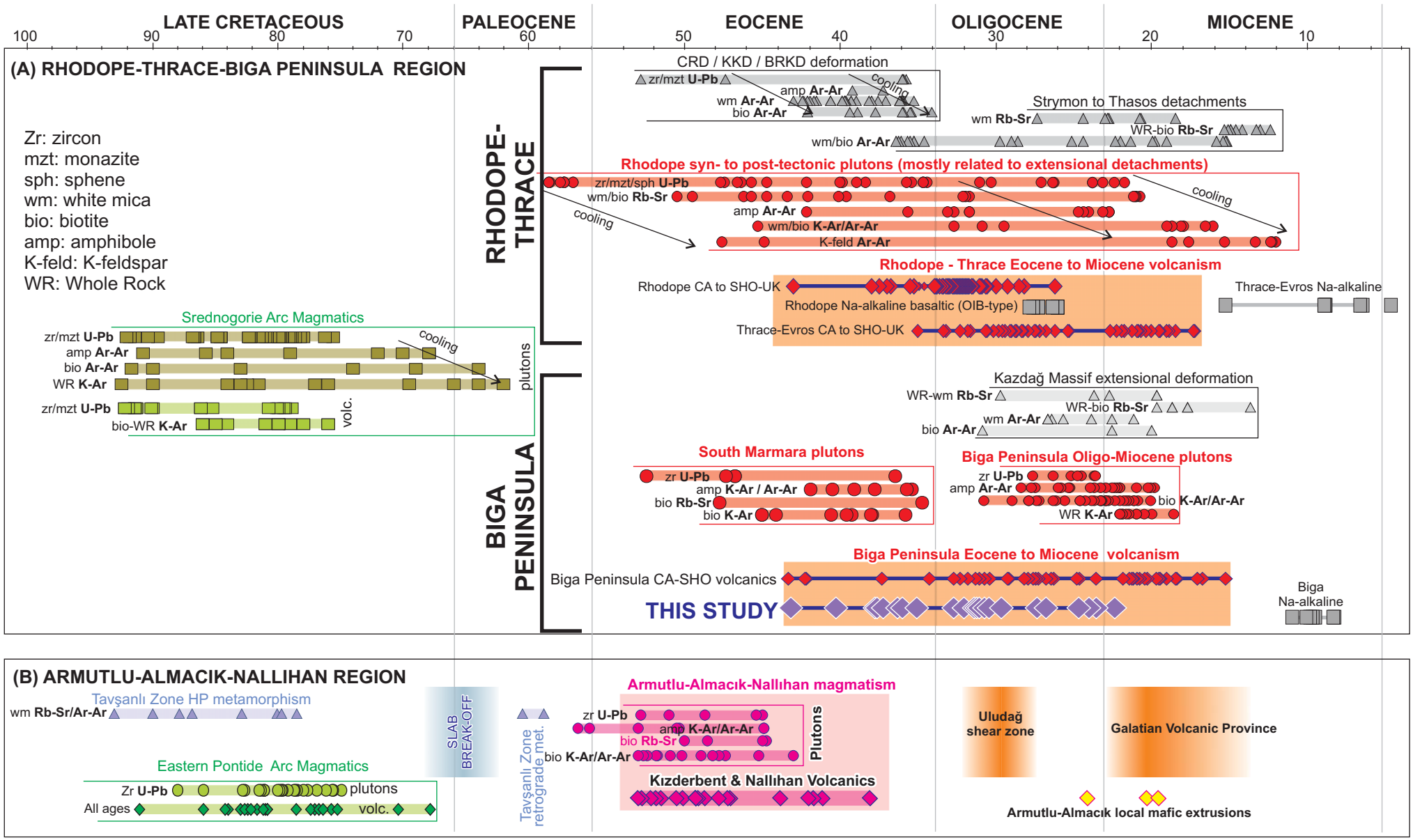
LATE CRETACEOUS
PALEOCENE
EOCENE
OLIGOCENE
MIOCENE
100
90
80
70
60
50
40
30
20
10
(A) RHODOPE-THRACE-BIGA PENINSULA REGION
Zr: zircon
mzt: monazite
sph: sphene
wm: white mica
bio: biotite
amp: amphibole
K-feld: K-feldspar
WR: Whole Rock
RHODOPE-THRACE
BIGA PENINSULA
CRD / KKD / BRKD deformation
zr/mzt U-Pb
amp Ar-Ar
wm Ar-Ar
bio Ar-Ar
cooling
Strymon to Thasos detachments
wm Rb-Sr
WR-bio Rb-Sr
wm/bio Ar-Ar
Rhodope syn- to post-tectonic plutons (mostly related to extensional detachments)
zr/mzt/sph U-Pb
wm/bio Rb-Sr
amp Ar-Ar
wm/bio K-Ar/Ar-Ar
K-feld Ar-Ar
Rhodope - Thrace Eocene to Miocene volcanism
Rhodope CA to SHO-UK
Rhodope Na-alkaline basaltic (OIB-type)
Thrace-Evros CA to SHO-UK
Thrace-Evros Na-alkaline
Srednogorie Arc Magmatics
zr/mzt U-Pb
amp Ar-Ar
bio Ar-Ar
WR K-Ar
plutons
bio-WR K-Ar
volc.
Kazdağ Massif extensional deformation
WR-wm Rb-Sr
WR-bio Rb-Sr
wm Ar-Ar
bio Ar-Ar
South Marmara plutons
zr U-Pb
amp K-Ar / Ar-Ar
bio Rb-Sr
bio K-Ar
Biga Peninsula Oligo-Miocene plutons
zr U-Pb
amp Ar-Ar
bio K-Ar/Ar-Ar
WR K-Ar
Biga Peninsula Eocene to Miocene volcanism
Biga Peninsula CA-SHO volcanics
THIS STUDY
Biga Na-alkaline
(B) ARMUTLU-ALMACIK-NALLIHAN REGION
Tavşanlı Zone HP metamorphism
wm Rb-Sr/Ar-Ar
SLAB BREAK-OFF
Tavşanlı Zone retrograde met.
Armutlu-Almacık-Nallıhan magmatism
zr U-Pb
amp K-Ar/Ar-Ar
bio Rb-Sr
bio K-Ar/Ar-Ar
Plutons
Kızderbent & Nallıhan Volcanics
Uludağ shear zone
Galatian Volcanic Province
Eastern Pontide Arc Magmatics
Zr U-Pb
plutons
All ages
volc.
Armutlu-Almacık local mafic extrusions

Figure 11

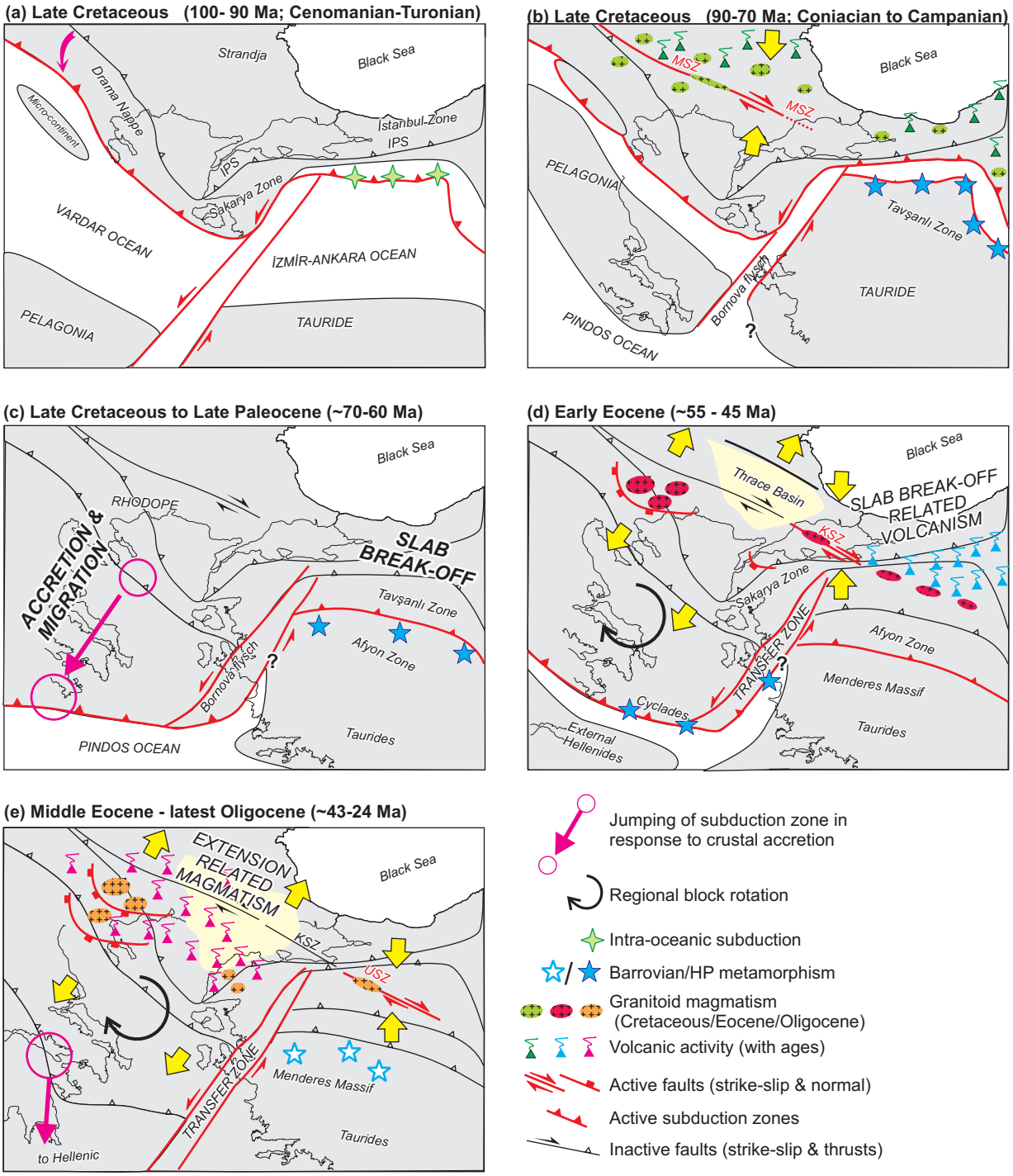
(a) Late Cretaceous (100- 90 Ma; Cenomanian-Turonian)
Strandja
Black Sea
Drama Nappe
Micro-continent
İstanbul Zone
IPS
IPS
Sakarya Zone
VARDAR OCEAN
İZMİR-ANKARA OCEAN
PELAGONIA
TAURIDE
(b) Late Cretaceous (90-70 Ma; Coniacian to Campanian)
MSZ
MSZ
Black Sea
PELAGONIA
Tavşanlı Zone
Bornova flysch
TAURIDE
PINDOS OCEAN
?
(c) Late Cretaceous to Late Paleocene (~70-60 Ma)
Black Sea
RHODOPE
ACCRETION & MIGRATION
SLAB BREAK-OFF
Tavşanlı Zone
Afyon Zone
Bornova flysch
?
Taurides
PINDOS OCEAN
(d) Early Eocene (~55 - 45 Ma)
Black Sea
Thrace Basin
SLAB BREAK-OFF RELATED VOLCANISM
KSZ
Sakarya Zone
TRANSFER ZONE
Afyon Zone
?
Menderes Massif
Cyclades
Taurides
External Hellenides
(e) Middle Eocene - latest Oligocene (~43-24 Ma)
EXTENSION RELATED MAGMATISM
Black Sea
KSZ
USZ
Menderes Massif
TRANSFER ZONE
Taurides
to Hellenic
Jumping of subduction zone in response to crustal accretion
Regional block rotation
Intra-oceanic subduction
Barrovian/HP metamorphism
Granitoid magmatism (Cretaceous/Eocene/Oligocene)
Volcanic activity (with ages)
Active faults (strike-slip & normal)
Active subduction zones
Inactive faults (strike-slip & thrusts)

Supplementary material 1

Click here to download Supplementary material for online publication only: Supplementary Material - 1.xls

Supplementary material 2

Click here to download Supplementary material for online publication only: Supplementary Material - 2.xls